Published in : Microbiological Research, vol. 285, August 2024
DOI: 10.1016/j.micres.2024.127745
Status : Postprint (Author's version)

Identification and genomic insights into a strain of *Bacillus velezensis* with phytopathogen-inhibiting and plant growth-promoting properties

Xiaoyan Liang[a, d], Shumila Ishfaq[a], Yang Liu[c], M. Haissam Jijakli[d], Xueping Zhou[b], Xiuling Yang[b, *], Wei Guo[a, *]

[a]Institute of Food Science and Technology, Chinese Academy of Agricultural Sciences/Key Laboratory of Agro-products Quality and Safety Control in Storage and Transport Process, Ministry of Agriculture and Rural Affairs, Beijing 100193, China

[b]State Key Laboratory for Biology of Plant Diseases and Insect Pests, Institute of Plant Protection, Chinese Academy of Agricultural Sciences, Beijing 100193, China

[c]School of Food Science and Engineering, Foshan University/National Technical Center (Foshan) for Quality Control of Famous and Special Agricultural Products (CAQS-GAP-KZZX043)/Guangdong Key Laboratory of Food Intelligent Manufacturing, Foshan 528231, Guangdong, China

[d]Gembloux Agro-Bio Tech, Liege University, Laboratory of Integrated and Urban Plant Pathology, Passage des déportés 2, 5030 Gembloux, Belgium

*Corresponding Author

Email: guowei01@caas.cn or iewguo@126.com (W. Guo); yangxiuling@caas.cn (X. L. Yang)

Tel: +86-10-62815925

Fax: +86-10-62815925

Published in : Microbiological Research, vol. 285, August 2024
DOI: 10.1016/j.micres.2024.127745
Status : Postprint (Author's version)

Abstract

The use of biological agents offers a sustainable alternative to chemical control in managing plant diseases. In this study, *Bacillus velezensis* IFST-221 was isolated from the rhizosphere of a healthy maize plant amidst a population showing severe disease symptoms. The investigation demonstrated a broad-spectrum antagonistic activity of IFST-221 against eight species of pathogenic ascomycetes and oomycetes, suggesting its potential utility in combating plant diseases like maize ear rot and cotton Verticillium wilt. Additionally, our study unveiled that IFST-221 has demonstrated significant plant growth-promoting properties, particularly in maize, cotton, tomato, and broccoli seedlings. This growth promotion was linked to its ability to produce indole-3-acetic acid, nitrogen fixation, phosphate and potassium solubilization, and biofilm formation in laboratory conditions. A complete genome sequencing of IFST-221 yielded a genome size of 3.858 M bp and a GC content of 46.71%. The genome analysis identified 3,659 protein-coding genes, among which were nine secondary metabolite clusters with known antimicrobial properties. Additionally, three unknown compounds with potentially novel properties were also predicted from the genomic data. Genome mining also identified several key genes associated with plant growth regulation, colonization, and biofilm formation. These findings provide a compelling case for the application of *B. velezensis* IFST-221 in agricultural practices. The isolate's combined capabilities of plant growth promotion and antagonistic activity against common plant pathogens suggest its promise as an integrated biological agent in disease management and plant productivity enhancement.

Keywords: *Bacillus velezensis*, antifungal activity, plant growth promotion, rhizobacterium, genomic analysis

Published in : Microbiological Research, vol. 285, August 2024
DOI: 10.1016/j.micres.2024.127745
Status : Postprint (Author's version)

1 Introduction

Maize (*Zea mays* L.), a staple grain crop for both human and livestock consumption, faces significant threats from insects and pathogens, with ear and stalk rot caused by *Fusarium verticillioides* being among the most destructive. This pathogen can infect plants from the roots, spreading through the stalk and reaching the ear and kernels, leading to reduced yields and potential secondary infection (Gai et al., 2018). This disease not only results in a reduction in maize yield but also poses a threat to human and livestock health by producing mycotoxins (Li et al., 2019; Savary et al., 2019). Compounding the problem, *F. verticillioides* produces mycotoxins such as Fumonisin B_1 (FB_1), classified by the International Agency for Research on Cancer (IARC), as a group 2B carcinogen, posing serious health risks to livestock and humans (Kujawa, 1994).

To combat maize ear and stalk rot, growers typically employ a mix of resistant cultivars, field management practices, and the application of chemical pesticides. However, it has been found that the resistance observed in specific cultivars under ideal experimental conditions may not be adequate for effectively managing the disease in the field (Dinolfo et al., 2022). Moreover, the excessive reliance on chemical fungicides for maize disease control has resulted in the emergence of resistance in certain fungal species. Additionally, this heavy use of chemicals raises environmental contamination and potential health risks for humans and animals (Pereira et al., 2021). Consequently, there's a growing demand for more sustainable solutions. Biological control methods, which rely on beneficial organisms to combat plant pathogens, present a promising alternative. They offer an environmentally and human-friendly approach to managing plant diseases, providing a sustainable path for controlling maize ear and stalk rot (González-Estrada et al., 2021; Gupta et al., 2021b).

Plant growth-promoting rhizobacteria (PGPR) inhabit the rhizosphere, a narrow soil zone surrounding plant roots, where they provide various benefits to plant development

Published in : Microbiological Research, vol. 285, August 2024
DOI: 10.1016/j.micres.2024.127745
Status : Postprint (Author's version)

(Kloepper et al., 1980). By colonizing plant roots, PGPR acts as a biofertilizer and biological control agent, protecting against a range of root pathogens, including bacteria, fungi, nematodes, and other harmful microorganisms (Haskett et al., 2020). A key group within this category is the genus *Bacillus*, renowned for its role in promoting plant growth and controlling pathogens. *Bacillus* species are capable of fixing atmospheric nitrogen, solubilizing phosphorus, and potassium, and enhancing nutrient uptake in plants (Gupta et al., 2021a). Moreover, these bacteria produce a range of phytohormones to stimulate plant growth like auxins, cytokinins, gibberellins, ethylene, and abscisic acid. *Bacillus* also produces some secondary metabolites which are crucial in preventing pathogen infection. Unlike primary metabolites, secondary metabolites are not essential for microbial growth and development but are synthesized in response to specific environmental conditions (Abdel-Aziz et al., 2017). They include various antibiotics, such as lipopeptides (surfactin, iturin, and fengycin), polyketides (macrolactin, bacillaene, and difficidin), and aminoglycoside (butirosin) can alter cell membrane structures and inhibit the growth of pathogenic fungi and bacteria (Heifetz et al., 1972; Harwood et al., 2018). In addition, lipopeptides produced by *Bacillus* can induce systemic resistance in plants leading to the production of defense-related proteins such as peroxidase, lipoxygenase, chitinase, and β-1,3-glucanase, which enhance the plant's resistance to the pathogens (Ongena et al., 2007; Lin et al., 2019; Tunsagool et al., 2019). Furthermore, *Bacillus* spp. can trigger the activation of enzymatic antioxidants crucial for plant defense, like phenylalanine ammonia-lyase and polyphenol oxidase (Wang et al., 2021). The chitinase and glucanase produced by *Bacillus* can degrade the fungal cell wall, directly inhibiting the growth of fungal hyphae (Tanaka and Watanabe, 1995).

Given the detrimental effects of *F. verticillioides* and its secondary metabolites, finding an eco-friendly method for disease management is crucial. In our investigation of maize ear and stalk rot in Yunan Province, it was observed that a healthy maize plant

Published in : Microbiological Research, vol. 285, August 2024
DOI: 10.1016/j.micres.2024.127745
Status : Postprint (Author's version)

in the vicinity of others with severely diseased symptoms. This unique observation prompted our study with the following objectives: (i) to isolate and identify the potential antifungal strains from the rhizosphere of the healthy maize plant; (ii) to evaluate the biocontrol effects against *Fusarium* ear and stalk rot as well as other fungal disease; (iii) to assess its growth-promoting activity in crop plants; (iv) to explore the mechanisms of its biocontrol and growth-promoting activities through genome mining and comparative genome analysis. By examining this strain's efficacy as a biocontrol agent and gaining insights into the genetic basis of its beneficial properties, this study aims to discover an effective biocontrol agent that can both enhance plant growth and manage fungal diseases in crops, contributing to sustainable agricultural practices.

2 Materials and methods

2.1 STRAINS

B. velezensis IFST-221 was isolated from the rhizosphere soil collected from maize in an area affected by *Fusarium* ear and stalk rot in Yunnan Province, China. Using a serial dilution method, 5 g of soil was mixed with 50 mL of 0.9% NaCl solution, and shaken at 30 °C for 30 minutes. A stepwise dilution (10^{-1}, 10^{-2}, 10^{-3}, 10^{-4}, 10^{-5}, 10^{-6}, and 10^{-7}) was carried out. For each dilution, 100 µL of solution was spread on Luria-Bertani (LB) medium and incubated at 30 °C for two days. After incubation, colonies were isolated and pure colony was obtained through streak plate preparation. To assess the strain's antifungal activity, a plate confrontation assay was performed. A 6 mm plug of *F. verticillioides* agar was placed in the center of the PDA plate and 5 µL of bacterial culture was carefully added on both sides of the fungal agar plug, approximately, 2.5 cm away. A control plate without bacterial culture was also prepared. All plates were incubated at 25 °C until the control plates exhibited full growth. The inhibition rate was calculated as inhibition rate (%) = (D1 – D2) / D2 ×100%, where D1 represents the diameter (mm) of the fungal colony in control and D2 represents the diameter (mm) of the fungal colony in the test plate. The experiment was conducted in triplicate and

Published in : Microbiological Research, vol. 285, August 2024
DOI: 10.1016/j.micres.2024.127745
Status : Postprint (Author's version)

repeated three times. *B. velezensis* IFST-221's antimicrobial spectrum was evaluated against seven additional phytopathogens *F. proliferatum*, *F. graminearum*, *F. oxysporum*, *F. solani*, *Botrytis cinerea*, *Phytophthora nicotianae*, and *Verticillium dahliae*. *Fusarium* strains used in this study were preserved in our laboratory and identified by morphological features and translation elongation factor 1α (*TEF-1α*) sequence, while non-*Fusarium* strains were also maintained in our laboratory and were identified based on the partial sequences of *ITS* (internal transcribed spacer region) gene.

2.2 IDENTIFICATION OF IFST-221

For identification, strain IFST-221 was subjected to morphological, biochemical, and molecular analysis. Colony morphology (color, shape, and surface) was observed on LB plate. Cell morphology was examined by scanning electron microscope (S-570, Hitachi, Japan). Biochemical analysis followed protocols outlined in "Bergey's Manual of Systematic Bacteriology" (Madigan et al., 2001), evaluating growth at various NaCl concentrations (2%, 5%, 7%, and 10%), pH tolerance at 5.7 and 6.8, temperature tolerance at 15 °C, 25 °C, 30 °C, 37 °C, and 40 °C. Catalase activity was assessed and utilization of various carbon sources (glucose, arabinose, xylose, mannitol, and starch) was examined. Citrate utilization, casein hydrolysis, the methyl red (MR) test, and the Voges Proskauer (VP) test were conducted to determine the strain's biochemical profile (Madigan et al., 2001). Additionally, the O-nitrophenyl-β-D-galactopyranoside (ONPG) test for identifying *B. velezensis* CR502^T was performed as described by Ruiz-García et al. (2005).

For molecular identification, the genomic DNA of IFST-221 was extracted using the TIANamp Bacteria DNA Kit (TIANGEN Biotech Co., Ltd., Beijing, China). The partial 16S rRNA gene was amplified using the primers 27F and 1492R (Chen et al., 2020), while the DNA gyrase subunit B (*gyrB*) gene was amplified using the primers

Published in : Microbiological Research, vol. 285, August 2024
DOI: 10.1016/j.micres.2024.127745
Status : Postprint (Author's version)

UP1 and UP2R (Yamamoto et al., 1995). The PCR reaction, in a 50 µL final volume, contained 25 µL Premix Taq (Takara Biomedical Technology Co., Ltd., Beijing, China), 1 µL forward primer and 1 µL reverse primer, 1 µL bacterial culture, and 22 µL ddH_2O under the 35 cycles of 94 °C for 10 sec, annealing at 55 °C for 30 sec, and 72 °C for 2 min. After amplification, products were separated using 1% agarose gel electrophoresis and purified with HiPure Gel Pure DNA Mini Kit (Magen Biotech, Guangzhou, China). Purified PCR products were then ligated into the pMD18-T vector (Takara Biomedical Technology Co., Ltd., Beijing, China), and transformed into *E. coli* TG-1. Positive transformants were selected and sequenced by Sangon Biotech (Shanghai) Co., Ltd. using Sanger sequencing. The resulting gene sequences of 16S rRNA and *gyrB* were aligned manually. Phylogenetic analysis of partial 16S rRNA and *gyrB* gene sequences was performed separately using MEGA X, respectively. The neighbor-joining method was employed to construct the phylogenetic trees. Evolutionary distances were calculated with the Kimura two-parameter model, and bootstrap analysis with 1000 replications was used to estimate the robustness of tree branches.

2.3 *IN VIVO* ANTI-*F. VERTICILLIOIDES* ASSAY OF IFST-221

To assess the inhibitory effect of IFST-221 on *F. verticillioides* in maize, *in vivo* assays were conducted using maize ears and kernels. For the maize ears assay, the front husks of maize ears were carefully removed, and the ears were sprayed with 2 mL IFST-221 culture at a concentration of 1×10^9 CFU/mL. A control group was treated with the same volume of distilled water (ddH_2O). Three days later, the maize ears were inoculated with either 10 µL of *F. verticillioides* conidial suspension with a concentration of 1×10^6 conidia/mL or ddH_2O for the control. Following the inoculation, the maize ears were re-covered with the removed husks, placed in a box with wet paper towels at the bottom to maintain humidity, wrapped with plastic wrap, and incubated in the dark at 25 °C for five days. The experiment was performed in triplicate and repeated

Published in : Microbiological Research, vol. 285, August 2024
DOI: 10.1016/j.micres.2024.127745
Status : Postprint (Author's version)

three times.

To evaluate the antifungal activity of *B. velezensis* IFST-221 against *F. verticillioides* in maize kernels, sterilized maize kernels were prepared following the method described by Liang et al. (2022). Fifteen sterilized maize kernels were immersed in either 10 mL *B. velezensis* IFST-221 culture at a concentration of 1×10^9 CFU/mL or ddH_2O. After one hour, the immersed maize kernels were inoculated with either 10 µL of *F. verticillioides* conidial suspension or ddH_2O. Each treatment was conducted five times and repeated in triplicate. The kernels were then incubated for five days, and symptoms of infection were observed and photographed.

To measure the relative fungal biomass in maize kernels, quantitative PCR (qPCR) was conducted following the protocol outlined by Zhang et al. (2023). The *β-tubulin* gene from *F. verticillioides* (*Fv_β-tubulin*) and the *gyrB* gene from *B. velezensis* (*Bv_gyrB*) were used to quantify fungal and bacterial colonization, respectively. The *translation elongation factor 1α* gene of maize (*Zm_TEF-1α*) served as endogenous plant control. The qPCR was conducted using SYBR Green (NovoStart® SYBR qPCR SuperMix Plus, Suzhou, China) on a Quant Studio™ 6 Flex System Cycler (Applied Biosystems, Waltham, MA, USA). The experiment was performed in triplicate to ensure the robustness and accuracy of the data. The specific primer sequences used for the qPCR analysis are listed in Supplementary Table S2.

The content of FB_1 in maize kernels was quantified by SAX solid-phase extraction and high-performance liquid chromatography coupled with mass spectrometry (HPLC-MS) with slight modifications (Ding et al., 2023). Briefly, crude fumonisin was extracted by homogenizing 5 g of ground maize kernels in 20 mL of acetonitrile/water (50:50, v/v) for 30 min followed by centrifugation at 4000 rpm for 5 min. the supernatant (3mL) was mixed with 8 mL methanol/water solution (60:20, v/v) and passed through SAX solid-phase extraction column (SAX-06-500mg, Bioland, China). Subsequently, the column was rinsed with 8 mL of methanol/water solution, 3 mL of

Published in : Microbiological Research, vol. 285, August 2024
DOI: 10.1016/j.micres.2024.127745
Status : Postprint (Author's version)

methanol, and 10 mL of methanol/acetic acid solution (99:1, v/v). The elution buffer was collected, evaporated, and dissolved in 1 mL of acetonitrile/water (20:80, v/v). After filtering through a 0.22 μm membrane, the samples were subjected to HPLC-MS/MS analysis. For HPLC-MS/MS analysis, 2 μL of the processed sample was injected into a Waters 2695 separation module (Waters Corporation, Milford, MA, USA) equipped with an EC-C18 reverse-phase column (100 mm × 2.1 mm, 1.7 μm). The mobile phase consisted of 0.1 % formic acid in water (solvent A) and acetonitrile (solvent B, 50:50, v/v) with a flow rate of 0.3 mL/min. The column was maintained at 35 °C during the analysis. FB_1 in the samples was identified and quantified by comparing retention times with FB_1 standards (Sigma-Aldrich Co., St Louis, MO).

2.4 THE BIOCONTROL ACTIVITY OF IFST-221 AGAINST *VERTICILLIUM* WILT OF COTTON

To evaluate the effectiveness of IFST-221 in combating *Verticillium* wilt in cotton, an experiment using a root-dipping method described by Zhang et al. (2020) was conducted. Cotton plants, aged three weeks, were divided into two groups. One group of 28 plants was treated with a 40 mL culture of IFST-221 at a concentration of 1×10^9 CFU/mL and the other group of 28 plants was treated with an equal volume of ddH_2O. After three days, both groups of 14 cotton plants were inoculated with a 20 mL suspension of *V. dahliae* conidia containing 5×10^6 conidia/mL, effectively introducing the pathogen into the plant roots. The other 14 cotton plants of both groups were inoculated with 20 mL ddH_2O. The experiment was repeated three times, and the severity of *Verticillium* wilt was evaluated based on disease incidence (DI) and disease severity index (DSI) as described by Zhu et al. (2013).

2.5 PLANT GROWTH-PROMOTING ASSAYS

In the pot experiments, all the maize, cotton, tomato, and broccoli seeds were purchased from the market. For each experiment, four 9 cm square plant pots were

Published in : Microbiological Research, vol. 285, August 2024
DOI: 10.1016/j.micres.2024.127745
Status : Postprint (Author's version)

prepared with five seeds planted in each pot. IFST-221 was cultured in LB liquid medium at 37 °C. The bacterial concentration of 1×10^9 CFU/mL. When the seedlings reached the two-leaf stage, a treatment of 40 mL of IFST-221 culture was added into each pot, while the fertilizer Huabao No. 2 (HYPONeX, America) was used as a control. Following a 30-day growth period, several growth metrics were assessed by measuring the height, root length, and fresh and dry weight of both the aboveground and underground parts of each plant.

In vitro studies were designed to evaluate the nitrogen-fixing, phosphorus- and potassium-solubilizing ability of IFST-221. A single colony of IFST-221 was cultured individually in a nitrogen-free medium to evaluate the nitrogen-fixing ability. Phosphorus solubilizing capacity was tested using the National Botanical Research Institute's phosphate growth medium (NBRIP), where the insoluble phosphorus source was $Ca_3(PO_4)_2$. Potassium solubilization was assessed with potassium feldspar powder as the insoluble potassium source in a potassium bacteria medium. These cultures were maintained at 30 °C for approximately 3-7 days, as described in previous studies (Chen et al., 2011; Ma et al., 2013; Nautiyal et al., 1999). The culture medium without inoculation served as a control.

For assessing indole-3-acetic acid (IAA) production, the Salkowski reaction was used with slight modifications (Fierro-Coronado et al., 2014). Briefly, a single colony of IFST-221 was cultured in LB medium supplemented with 100 mg/L L-tryptophan and incubated at 37 °C for two days. After centrifugation, 2 mL of the supernatant was mixed with an equal volume of Salkowski regent and kept in the dark for 30 min. The absorbance of the resulting solution was measured at 530 nm using a spectrophotometer. The concentration of IAA production was estimated by comparing the absorbance with an IAA standard curve. The experiment was conducted in triplicate and repeated three times to ensure the reliability of the results.

Published in : Microbiological Research, vol. 285, August 2024
DOI: 10.1016/j.micres.2024.127745
Status : Postprint (Author's version)

2.6 GENOMIC SEQUENCING, ANNOTATION, AND PREDICTION OF SECONDARY METABOLITES

The genome of IFST-221 was sequenced using Single Molecule Real-Time (SMRT) technology. This sequencing work was conducted by Beijing Novogene Bioinformatics Technology Co., Ltd (Beijing, China).To maintain data integrity, low-quality reads were filtered using SMRT Link v5.0.1, resulting in high-quality contigs. The assembly produced a single continuous contig without any gaps, indicating a high-quality genome assembly. For comparative analysis, the genomic sequences of related strains including *B. velezensis* SQR9 (NZ_CP006890.1), *B. velezensis* FZB42^T (NC_009725.2), *B. amyloliquefaciens* DSM7^T (NC_014551.1), and *B. subtilis* 168^T (NC_000964.3) were downloaded from NCBI website. These sequences were used as references to compare and analyze the genomic features and characteristics of IFST-221.

Various software tools were employed to perform comparative analyses and gene annotation. The BLAST Ring Image Generator (BRIG) 0.95 software was used to visualize genomic comparisons among the five *Bacillus* strains (Alikhan et al., 2011), while collinearity analysis was performed using TBtools-II (Chen et al., 2023). Whole-genome orthologous gene comparisons were done using OrthoVenn 2 (Xu et al., 2019). The coding sequence (CDS) of *B. velezensis* IFST-221, SQR9, and FZB42^T, *B. amyloliquefaciens* DSM7^T, and *B. subtilis* 168^T were used for this analysis. The related coding genes of IFST-221 were analyzed by BLAST search with specific parameters (E-value less than 1e-5, minimal alignment length percentage larger than 40%). After comparative analysis, the singletons in IFST-221 were annotated using eggNOG-mapper (Cantalapiedra et al., 2021). Gene annotation and function prediction were performed using a combination of GeneMarkS, Gene Ontology (GO), Kyoto Encyclopedia of Genes and Genomes (KEGG), and Clusters of Orthologous Groups (COG) databases. To identify secondary metabolites, the genome sequence of IFST-221 was analyzed with the antiSMASH 6.0 website, and the default settings were applied for prediction.

Published in : Microbiological Research, vol. 285, August 2024
DOI: 10.1016/j.micres.2024.127745
Status : Postprint (Author's version)

2.7 DATA AVAILABILITY

The genomic sequence of IFST-221 is available at the NCBI website with accession No. CP125283.1.

3 Results

3.1 ISOLATION OF AN ANTIFUNGAL STRAIN IFST-221

To explore potential sources of disease resistance in maize, soil suspension from healthy maize rhizosphere in Yunnan Province was shaken at 30 °C for 20 min. Following a stepwise dilution method, a total of 156 strains were isolated. These strains were tested for their antifungal activity against *F. verticillioides* to identify potential disease resistance. IFST-221 exhibited the highest antifungal potential, inhibiting 62.63% of *F. verticillioides*. To further assess the broad-spectrum antimicrobial activity of IFST-221, additional tests were conducted using various phytopathogens including *F. proliferatum*, *F. graminearum*, *F. oxysporum*, *F. solani*, *B. cinerea*, *P. nicotianae*, and *V. dahliae*. The results revealed that IFST-221 exhibited robust antagonistic effects against all the tested pathogens, with relatively broad-spectrum activity against both ascomycetes and oomycetes are shown in Figure 1A. Inhibition rates of up to 77.88% were observed against *P. nicotianae*, and up to 60% against other tested pathogens (Fig. 1B).

Scanning electron microscopy (SEM) was employed to examine the ultrastructural effect of IFST-221 on fungal hyphae, focusing on strains such as *F. verticillioides*, *B. cinerea*, *P. nicotianae*, and *V. dahliae* were examined. SEM images of untreated *F. verticillioides* hyphae displayed smooth surfaces and intact hyphae. However, when treated with IFST-221, the hyphae exhibited notable morphological changes, appearing folded, twisted, and partially distended (Fig. 1C). Similarly, irregular hyphae structures were observed in IFST-221 treated other pathogens (Fig. 1C). These findings suggest

Published in : Microbiological Research, vol. 285, August 2024
DOI: 10.1016/j.micres.2024.127745
Status : Postprint (Author's version)

that treatment with IFST-221 induces morphological alterations in the hyphae of the tested pathogens.

3.2 IFST-221 is a strain of *B. velezensis*

To determine the taxonomic classification of IFST-221, its morphology was initially examined. When cultured on the LB solid medium, a single colony of IFST-221 displayed characteristics such as being round, opaque, milky white to yellow, and possessing folded edges. Gram staining revealed that IFST-221 was a gram-positive bacterium, indicated by the purple color from crystal violet dye. SEM revealed that IFST-221 is a rod-shaped bacterium with a width ranging from 0.2-0.25 μm and a length ranging from 0.6-1.2 μm (Fig. S1). To gain further insights into the physiological and biochemical characteristics of IFST-221, tests outlined in "Bergey's Manual of Systematic Bacteriology" were conducted. IFST-221 exhibited positive results in various tests, including catalase activity, carbon sources utilization based on dextrose, arabinose, xylose, mannitol, and starch, citrate utilization, casein hydrolysis, MR test, and VP test. Moreover, IFST-221 demonstrated the ability to thrive under a range of growth conditions, including tolerating NaCl concentrations between 2% to 7%, pH levels ranging from 5.7 to 6.8, and temperatures within the range of 15 to 40 °C (Table S1). These findings collectively indicate that the IFST-221 belongs to the *Bacillus* group.

To ensure precise identification of the *Bacillus* strain IFST-221, a molecular phylogeny analysis was conducted. This method could overcome the limitations inherent in relying solely on morphological and physiological characteristics. The analysis focused on key genetic markers, particularly the 16S rRNA gene, a well-established marker for determining bacterial phylogenetic relationships. Comparing the 16S rDNA gene sequence of IFST-221, which had a length of 1512 bp to sequences from known *Bacillus* species revealed that IFST-221 shared up to 99% identity with

Published in : Microbiological Research, vol. 285, August 2024
DOI: 10.1016/j.micres.2024.127745
Status : Postprint (Author's version)

the aligned type strains of different *Bacillus* species, including *B. subtilis* subsp. *spizizenii*, *B. rugosus*, *B. tequilensis*, *B. cabrialesii*, *B. inaquosorum*, *B. vallismortis*, *B. amyloliquefaciens*, *B. nematocida*, *B. velezensis*, and so on (Fig. S2). This high degree of sequence similarity suggested a close relationship between IFST-221 and these *Bacillus* species. The phylogenetic analysis further confirmed a close relationship between IFST-221 and *B. velezensis* strains NRRL B-41580^T and BCRC 17467^T, but not CR-502^T (Fig. S2). This outcome, however, highlighted the potential limitation of using the 16S rDNA marker for accurately differentiating between closely related *Bacillus* species. Another phylogenetic marker, *gyrB* gene, which encoded the subunit B protein of DNA gyrase, was examined to provide additional clarity. The BLASTn analysis of *gyrB* sequences obtained from IFST-221 revealed a high level of identity, 98.87% with the type strain *B. velezensis* BCRC 17467^T. This strong similarity was further supported by the phylogenetic analysis, which showed that IFST-221 and *B. velezensis* BCRC 17467^T clustered together on the same branch (Fig. S3). Furthermore, the ONPG production test was conducted to distinguish *B. amyloliquefaciens* and *B. velezensis*. IFST-221 exhibited ONPG production like that of *B. velezensis* CR-502^T (Table S1). The combined results from the 16S rRNA and *gyrB* genes, as well as the ONPG production test, confirmed that IFST-221 is a strain of *B. velezensis*, providing a robust and multifaceted approach to the identification and classification of this strain.

3.3 *B. VELEZENSIS* IFST-221 IS A PUTATIVE BIOLOGICAL CONTROL AGENT FOR PLANT DISEASE

To evaluate the effectiveness of *B. velezensis* IFST-221 as a biological control agent, *in vivo* anti-phytopathogenic activity against *F. verticillioides* in maize ears and kernels. Maize ear and kernels were pre-sprayed with IFST-221 and ddH_2O before inoculating with *F. verticillioides*. The results showed a significant reduction in *F. verticillioides* infection in maize ears pre-sprayed with IFST-221 compared to those pre-sprayed with ddH_2O (Fig. 2A). Similarly, when maize kernels were pre-immersed in ddH_2O and then

Published in : Microbiological Research, vol. 285, August 2024
DOI: 10.1016/j.micres.2024.127745
Status : Postprint (Author's version)

inoculated with *F. verticillioides* exhibited visible hyphae formation, the kernels that were pre-immersed with IFST-221 and then inoculated with *F. verticillioides* did not show any visible fungal hyphae (Fig. 2B). The qPCR analysis supported these observations, indicating a considerable reduction in the biomass of *F. verticillioides* in kernels treated with IFST-221 compared to ddH_2O (Fig. 2C). Moreover, the treatment of maize kernels with IFST-221 resulted in a significant reduction in the production of FB_1, a mycotoxin produced by *F. verticillioides*, with levels dropping from 5700.33 parts per billion (ppb) per gram of maize kernels in the control group to 19.63 ppb in the IFST-221 treated group (Fig. 2D).

Similarly, IFST-221 demonstrated potential as a biocontrol agent against cotton Verticillium wilt (Fig. 2E and F). At 30 days post inoculation of *V. dahliae*, cotton plants that were pre-treated with IFST-221 showed a significantly lower DSI (8.93%) compared to cotton plants without the pretreatment of IFST-221 (73.21%) (Fig. 2F). The disease incidence of cotton plants inoculated with *V. dahliae* and treated with IFST-221 was 14.29%, whereas the DI of plants without treatment was 85.71% (Fig. 2F). Furthermore, it is worth noting that cotton plants treated with IFST-221 exhibit better growth compared to those treated with ddH_2O (Fig. 2E).

3.4 *B. VELEZENSIS* IFST-221 PROMOTES PLANT SEEDLING'S GROWTH

To evaluate the potential of IFST-221 in promoting plant growth, experiments were conducted on maize, cotton, tomato, and broccoli seedlings with treatment and control groups. The treatment group was inoculated with IFST-221, while a commercial fertilizer served as the control. Plant growth was monitored over 30 days, and it was observed that the inoculation of IFST-221 resulted in a noticeable enhancement in plant growth as depicted in Figure 3A. After 30 days post-inoculation, there was a noticeable increase in plant height among treated plants. For maize, the average height was 11.57 ± 1.72 cm, compared to the control height of 10.17 ± 1.13 cm. Similarly, the height of

Published in : Microbiological Research, vol. 285, August 2024
DOI: 10.1016/j.micres.2024.127745
Status : Postprint (Author's version)

treated cotton increased to 13.67 ± 1.67 cm whereas the control group measured 11.30 ± 1.90 cm (Fig. 3B). Furthermore, all plants including maize, cotton, tomato, and broccoli, that were treated with IFST-221 showed a significant ($p < 0.05$) increase in fresh weight of the aboveground part (Fig. 3B). Moreover, in the case of broccoli, the dry weight of the aboveground part was significantly increased (0.37 ± 0.13 g) compared to the control treatment weight (0.19 ± 0.13 g).

Although treatment with IFST-221 didn't have a significant effect on the root length and the underground part of maize, tomato, and broccoli seedlings, it is worth noting that cotton treated with IFST-221 showed remarkable improvement (Fig. 3B). Specifically, compared to the control group, cotton plants treated with IFST-221 experienced a 0.5-fold increase in the fresh weight of the underground part and a 1.5-fold increase in root length (Fig. 3B). These findings suggest that IFST-221 plays a crucial role in enhancing the fresh weight of the aboveground part of the tested plant seedlings, especially cotton. Additionally, IFST-221 showed versatility by thriving in various nutrient-deficient cultures, suggesting its adaptability to different environmental conditions. This was observed in nitrogen-free cultures, NBRIP, and potassium bacteria medium, demonstrating that IFST-221 could grow in nutrient-limited environments (Figure 3C). Moreover, crystal violet staining of IFST-221 grown on LBGM medium revealed the formation of a wrinkled structure, a common phenotype observed in mature biofilms produced by various bacteria (Fig. 3D). Additionally, when IFST-221 was cultured for 12 hours, it produced 5.59 mg/L of IAA as determined by the Salkowski reagent method.

3.5 GENOMIC FEATURE OF *B. VELEZENSIS* IFST-221 AND COMPARATIVE GENOMICS ANALYSIS OF *B. VELEZENSIS* IFST-221, SQR9, FZB42^T, *B. AMYLOLIQUEFACIENS* DSM7^T, AND *B. SUBTILIS* 168^T

The whole genome sequencing of IFST-221 yielded significant insights into the genomic features. Following the sequencing and quality assessment of the original

Published in : Microbiological Research, vol. 285, August 2024
DOI: 10.1016/j.micres.2024.127745
Status : Postprint (Author's version)

reads, the assembled genome consisted of one contig with an N50 length of 3,874,945 base pair (bp). The entire genome of IFST-221 comprised a circular chromosome with a length of 3,858,300 bp and a GC content of 46.71% (Fig. 4A). Within this genome, a total of 3,973 genes were identified, accounting for approximately 90.06% of the total genome length with a combined gene length of 3,474,660 bp. Additionally, the genome analysis predicted the presence of 86 tRNA structures, nine rRNA operons (i.e., 5S, 16S, and 23S structures), and six sRNA were also predicted in the genome of IFST-221 (Table 1). The genome sequencing data of IFST-221 have been deposited in the National Center for Biotechnology Information (NCBI) under the GenBank BioProject number CP125283.1.

To deeply understand the genetic characteristics of IFST-221, a comparison of gene features was made using the nucleotide sequence of well-studied and standard *Bacillus* strains, including *B. velezensis* SQR9, *B. velezensis* FZB42^T, *B. amyloliquefaciens* DSM7^T, and *B. subtilis* 168^T. Compared to other strains, IFST-221 exhibited a smaller genome size, lower GC content, fewer CDS, less average CDS size, and a higher percentage of coding region (Table 1). Based on the Average Nucleotide Identity (ANI) value of these strains, it was confirmed that IFST-221 belongs to the *B. velezensis* strain because of the high ANI value between IFST-221 and *B. velezensis* SQR9 and FZB42^T (Fig. S4). Also, a collinearity analysis was performed to examine the genomic similarities and variations among five strains. The analysis revealed a generally collinear relationship among the genomes, indicating that the gene order and arrangement were largely conserved. Despite this overall collinearity, some genome rearrangement events, such as inversions and translocations, were observed among the five *Bacillus* genomes (Fig. 4B). Among these strains, IFST-221 showed the highest synteny with SQR9.

In addition to collinearity, a comprehensive protein sequence analysis using OrthoVenn2 was performed to compare the orthologous and paralogous clusters across

Published in : Microbiological Research, vol. 285, August 2024
DOI: 10.1016/j.micres.2024.127745
Status : Postprint (Author's version)

the five strains. Out of the 3,659 proteins identified in IFST-221, 3,542 clusters were generated by comparing orthologs and paralogs among the five *Bacillus* strains. Additionally, 90 singletons were observed, representing genes that did not have orthologs in other species (Fig. 4C and D). Additionally, 3,019 clusters were common to all five strains, indicating a significant overlap in genetic content (Fig. 4C). A total of 3,468 overlapping clusters were common between IFST-221 and *B. velezensis* SQR9. IFST-221 shared 3,424 clusters with *B. velezensis* FZB42^T and 3,358 clusters with *B. amyloliquefaciens* DSM7^T, while sharing 3,180 clusters with *B. subtilis* 168^T. Additionally, two unique clusters were identified for IFST-221 (Fig. 4C). These unique clusters contained four proteins (IFST-221_GM001075, IFST-221_GM001077, IFST-221_GM001080, and IFST-221_GM001084) involved in ATP and DNA binding, which were important biological processes. Furthermore, 90 singletons found in IFST-221 were annotated using eggNOG-mapper. The results revealed that ten proteins were associated with information storage and processing, eight proteins were involved in signal transduction and mechanisms, 12 proteins were associated with coenzyme transport and metabolism, and 60 proteins had unknown functions (Fig. 4D).

3.6 PREDICTION OF THE ANTIMICROBIAL CHARACTERISTIC OF IFST-221

Functional annotation of protein-coding genes is crucial for understanding the molecular functions of the species. In the case of IFST-221, 2,574, 3,810, and 2,846 protein-coding genes were annotated in the GO, KEGG, and COG database, respectively (Fig. S5). In the whole genome of IFST-221, 12 possible secondary metabolites gene clusters were predicted using the antiSMASH bacterial version (Table 2, Fig. 4A, and 4B). Among these clusters, three were predicted to encode unknown secondary metabolites through unknown clusters. However, cluster 1, cluster 2, cluster 3, cluster 4, cluster 5, cluster 6, cluster 7, cluster 8, and cluster 9 were associated with the production of surfactin, fengycin, bacillibactin, macrolactin H, difficidin,

Published in : Microbiological Research, vol. 285, August 2024
DOI: 10.1016/j.micres.2024.127745
Status : Postprint (Author's version)

bacillaene, bacilysin, butirosin A/B, and andalusicin A/B, respectively. This indicates that IFST-221 possesses genes responsible for the biosynthesis of surfactin, fengycin, bacillibactin, macrolactin H, difficidin, bacillaene, bacilysin, butirosin A/B, and andalusicin A/B. And andalusicin A/B is the one difference from secondary metabolites from the other four strains according to the antiSMASH prediction results (Table 2).

In addition, collinearity analysis was performed to analyze the consistency of 12 gene clusters among the five strains. The high similarity in the orders of secondary metabolite gene clusters among the five strains is depicted in Figure 4B. However, the genetic identity of these secondary metabolites showed differences. Based on the highlighted brown line, which indicates a high level of consistency among the five strains, the known gene clusters of butirosin, bacillibactin, and bacilysin exhibited a greater degree of consistency. Other gene clusters of predicted secondary metabolites, including andalusicin, surfactin, macrolactin, bacillaene, fengycin, and difficidin, showed more variation, indicating that these substances may be different from the other four related strains. Notably, three predicted unknown gene clusters, encoding unknown 1, 2, and 3, showed high conservation among the five strains. The similarity of gene clusters may partially explain the variations observed in the predicted secondary metabolites among the five strains.

3.7 GLOBALLY SCREENING OF GENES POTENTIALLY CONTRIBUTING TO PLANT GROWTH-PROMOTING ACTIVITIES IN IFST-221

The annotation results from eggNOG and GO databases offer valuable insights into the potential roles of genes within the IFST-221 genome, especially regarding plant growth promotion, colonization, and biofilm formation. In addition to the genes responsible for antimicrobial secondary metabolites production (*srf*, *fen*, *dhb*, *btr*, *bac*, *ancKC/anCMT*, *bae*, *mln*, and *dif*), there are numerous additional genes that directly or indirectly contribute to plant promotion (Fig. 5). IFST-221 possesses genes involved in

Published in : Microbiological Research, vol. 285, August 2024
DOI: 10.1016/j.micres.2024.127745
Status : Postprint (Author's version)

the synthesis of IAA through the indole-3-acetonitrile (IAN) pathway (*ysnE* and *yhcX*). Furthermore, IFST-221 carries the *phy* gene, which is responsible for phytase production. It also possesses the genes involved in acquiring and utilizing PO_4^{3-} (*pstABCS*), K^+ (*ackA*, *gltA*, and *mdh*), Fe^{3+} (*yclNOPQ*), and N_2 (*nifU*). The synthesis of plant cell wall-degrading enzymes is another important trait for colonization in the rhizosphere. IFST-221 carries genes such as *bglC5*, *bglS*, and *yhfE* involved in the coding of endo-β-glucanase, *bglA* and *licH* related to endo-β-glucosidase, Additionally, IFST-221 possesses genes (*xylA/B* and *xynA/B)* involved in the coding of xylanase. Moreover, IFST-221 genome contains a complete pathway for biofilm formation, including *kinC/D*, *spo0A*, *abbA*, *abrB*, *sinI/R*, *eps*, and *yqxM/tapA-sipW-tasA*, as described in Yu et al. (2016). Overall, the comprehensive analysis of the IFST-221 genome demonstrates its potential as a biological control agent and hopefully enables its use in the future with capabilities in plant growth promotion, colonization, and biofilm formation.

4 Discussion

Plant growth-promoting rhizobacteria (PGPR) play a dual role in agriculture, serving as biocontrol agents that protect plants from pathogens and offering a range of benefits to crops, such as stimulating growth, boosting yields, enhancing seedling vigor, and aiding seed germination (Tabassum et al., 2017). In this study, we isolated and identified *B. velezensis* IFST-221 from the healthy maize rhizosphere in the field experiencing a high incidence of *Fusarium* ear and stalk rot. The IFST-221 exhibited broad-spectrum antimicrobial activity against oomycetes and ascomycetes *in vitro*. When applied to crops, IFST-221 treatment resulted in a remarkable alleviation of both maize ear rot and cotton Verticillium wilt. Moreover, seedlings of maize, cotton, tomato, and broccoli treated with IFST-221 showed enhanced growth compared to untreated seedlings, indicating its potential as a plant growth regulator. Thus, *B.*

Published in : Microbiological Research, vol. 285, August 2024
DOI: 10.1016/j.micres.2024.127745
Status : Postprint (Author's version)

velezensis IFST-221 emerges as a promising PGPR candidate for sustainable agriculture, offering both disease control and plant growth benefits.

For a significant period, *B. velezensis* was considered as a later heterotypic synonym of *B. amyloliquefaciens* (Wang et al., 2008; Borriss et al., 2011). However, in 2016, it was recognized as a separate species from *B. amyloliquefaciens*. In 2017, *B. amyloliquefaciens*, *B. velezensis*, and *B. siamensis* were classified as an "operational group *B. amyloliquefaciens*" within the *B. subtilis* species complex (Dunlap et al., 2016; Fan et al., 2017). Although the 16S rRNA gene is commonly used to determine bacterial phylogenetic relationships, it has proven a bit unreliable for differentiating closely related *Bacillus* species, largely due to the high sequence similarity among these species. This limitation is demonstrated in the phylogenetic analysis of the 16S rRNA gene sequence of *B. velezensis* IFST-221 compared with other *Bacillus* species. Instead, the *gyrB* gene has emerged as a more reliable alternative to the 16S rRNA gene for identifying and analyzing members of the *B. subtilis* group (Wang et al., 2007). In the phylogenetic analysis, the *gyrB* gene sequence of IFST-221 formed a distinct branch alongside the type strain *B. velezensis* BCRC 17467^T, providing evidence that IFST-221 belongs to the *B. velezensis* species. Additional support for this conclusion came from the ONPG test and the comparative analysis of genomic features. The analysis revealed a higher ANI value and a greater number of shared gene clusters between IFST-221 and *B. velezensis* SQR9 and FZB42^T (Fig. 4B, C, and Fig. S4).

The *Bacillus* genus, especially *B. velezensis*, has garnered considerable interest for its production of various antimicrobial secondary metabolites (Chowdhury et al., 2015). FZB42^T, isolated from the maize rhizosphere, was the first strain in this group to have its genome annotated (Chen et al., 2007). Since then, an increasing number of *B. velezensis* species have been isolated from rhizospheres of different plants, such as tomato, wheat, cucumber, polar, and lettuce. As of 2024/04/25, there are 859 genome assembly and annotation reports of *B. velezensis* available in the NCBI database. It is

Published in : Microbiological Research, vol. 285, August 2024
DOI: 10.1016/j.micres.2024.127745
Status : Postprint (Author's version)

worth noting that different *Bacillus* strains exhibit variation in the production of antimicrobial secondary metabolites. These metabolites typically fall into the categories of polyketides and non-ribosomal synthetic peptides. Polyketides such as bacillaene, macrolactin, and difficidin are synthesized by polyketide synthase gene clusters *bae* (formerly *pks1*), *mln* (formerly *pks2*), and *dif* (formerly *pks3*) (Chen et al., 2006). Non-ribosomal peptide synthetases (NRPS) produce numerous lipopeptides, including iturins, surfactins, fengycins, and bacillibactin (Mongkolthanaruk, 2012; Cochrane and Vederas, 2016). Though both IFST-221 and FZB42^T were isolated from the maize rhizosphere, their secondary metabolite profiles differ. Both strains produce antimicrobial substances including surfactin, fengycin, bacillibactin, macrolactin H, difficidin, bacillaene, bacilysin, and butirosin A/B. However, FZB42^T was predicted to produce plantazolicin, bacillothiazol, and three other substances, whereas IFST-221 was predicted to produce andalusicin A/B and three other unknown substances (Table 2). Interestingly, the IFST-221 has a smaller genome size but comparatively higher GC content than *B. velezensis* SQR9, FZB42^T, *B. amyloliquefaciens* DSM7^T, and *B. subtilis* 168^T. These findings suggest that IFST-221 may possess a higher denaturation temperature and enhanced tolerance to harsh environmental conditions.

Collinearity analysis has demonstrated that the secondary metabolites gene clusters become more compact as evolution progresses through the five strains, from *B. subtilis* 168, *B. amyloliquefaciens* DSM7^T, to *B. velezensis* FZB42^T, SQR9, and IFST-221 (Fig. 4B). This evidence suggests that IFST-221 may retain more secondary metabolite genes as an adaptation to survive in a harsher environment. Additionally, this adaptation includes targeted deletions and integrations of less important genes as an adaptive response. Among the predicted secondary metabolites, IFST-221 produces a unique chemical called andalusicin A/B, which belongs to class III lanthipeptide, which is the well-known family of ribosomally synthesized and post-translationally modified peptides, was also reported to inhibit the growth of Gram-positive bacteria (Grigoreva

Published in : Microbiological Research, vol. 285, August 2024
DOI: 10.1016/j.micres.2024.127745
Status : Postprint (Author's version)

et al., 2021). Considering that the other predicted secondary metabolites, such as surfactin, fengycin, bacillibactin, macrolactin, difficidin, bacillaene, and bacilysin, have been successfully extracted from *B. velezensis* SQR9 using reverse-phase high-pressure liquid chromatography analysis *in vitro* (Xu et al., 2013; Li et al., 2014; Wu et al., 2018), it is reasonable to assume that similar methods could be used to extract and produce secondary antimicrobial metabolites from IFST-221 for further studies. Notably, even though most of the predicted secondary metabolites align with those found in other *B. velezensis*, the results of the gene variation in the collinearity analysis suggest the possibility of discovering novel compounds in IFST-221.

In the pot experiment, IFST-221 exhibited the ability to promote the growth of maize, cotton, tomato, and broccoli seedlings. Plants treated with IFST-221 resulted in a significant increase in plant height and fresh weight of the aboveground part compared to control groups (Fig. 3). This growth-promoting effect is partly attributable to the presence of IAA in the culture of IFST-221, indicating that it may synthesize IAA. Bacteria can produce IAA through various pathways using L-tryptophan (Trp), including the indole-3-acetamide (IAM) pathway, indole-3-pyruvic acid (IPyA) pathway, tryptophan side-chain oxidase (TSO) pathway, tryptamine (TAM) pathway, and indole-3-acetonitrile (IAN) pathway (Keswani et al., 2020). In the IFST-221 genome, the IAOD (acetaldoxime dehydratase) encoded by *ysnE* and nitrilase (indole-3-acetonitrile nitrilase) encoded by *yhcX* are present, which convert Trp to IAA. However, some genes associated with the other four pathways are absent. The *nif* gene cluster plays a vital role in biological nitrogen fixation with *nifU* and *nifS* encoding components of the nitrogen fixation-specific iron-sulfur cluster assembly pathway (Ryu et al., 2020). Although *nifU* is not essential for all nitrogen-fixation strains (Wang et al., 2013), its presence indicates potential nitrogen-fixation capabilities. IFST-221 also possesses features characteristic of plant growth-promoting rhizobacteria (PGPR), such as the ability to solubilize insoluble phosphate and potassium. Genomic mining and *in*

Published in : Microbiological Research, vol. 285, August 2024
DOI: 10.1016/j.micres.2024.127745
Status : Postprint (Author's version)

vitro experiments confirmed these traits in IFST-221, with the *phy* gene encoding phosphohydrolase, or phytase, for organic phosphate solubilization (Torres et al., 2023). Additionally, the high affinity phosphate transport system (*pst*) is essential for phosphate uptake in a nutrient-deficient environment (Moreno-Letelier et al., 2011). The ability of IFST-221 to solubilize potassium is supported by the upregulation of genes such as *ackA*, *gltA*, and *mdh* in potassium-solubilizing strain *B. aryabhattai* SK1-7 (Chen et al., 2022). Despite its various plant growth-promoting properties, the genome of *Bacillus velezensis* IFST-221 lacks the *ktrAB* and *ktrCD* genes, which encode the high-affinity and low-affinity potassium transporters, respectively. (Gundlach et al., 2017). While IFST-221's ability to secrete siderophores for iron acquisition wasn't observed in our study, the genome analysis revealed the presence of a bacillibactin (BB) biosynthesis pathway based on *dhb* gene cluster. In addition, the *yclNOPQ* operon encodes a complete transporter for petrobactin (PB), a photoreactive 3,4-catecholate siderophore (Zawadzka et al., 2009). Moreover, IFST-221 contains enzymes such as cellulases specialized in cellulose degradation, glucanase, and glucosidase involved in glucan degrading, which play a significant role in bacterial colonization of the rhizosphere of plants (Sritongon et al., 2023). Biofilm formation in IFST-221 adds to its ecological adaptability, enhancing its resilience in challenging environmental conditions. While these characteristics suggest that IFST-221 has the potential for plant growth promotion and rhizosphere colonization, the impact of IFST-221 on plant growth across various abiotic conditions has yet to be comprehensively evaluated. Despite this, the *in vitro* growth of IFST-221 in different nutrient-deficient cultures suggests its adaptability and potential for application in diverse environmental settings. Further studies will be needed to fully understand IFST-221's capabilities in promoting plant growth under different environmental conditions and its resilience against abiotic stresses.

Published in : Microbiological Research, vol. 285, August 2024
DOI: 10.1016/j.micres.2024.127745
Status : Postprint (Author's version)

5 Conclusion and future perspective

B. velezensis IFST-221 is a promising PGPR with a broad spectrum of antimicrobial activity and notable plant growth-promoting abilities. Comparative genomic analysis of IFST-221 and related strains revealed the presence of 12 secondary metabolites, including surfactin, fengycin, bacillibactin, macrolactin H, difficidin, bacillaene, bacilysin, butirosin A/B, andalusicin A/B, and three unknown secondary metabolites. Notably, the IFST-221 exhibited three unidentified secondary metabolites as well as a distinctly known metabolite, andalusicin A/B. Furthermore, the deep mining of IFST-221 genome has provided insights into the genetic potential for plant growth regulation, colonization, and biofilm formation. Overall, the characteristics and genomic features of *B. velezensis* IFST-221 indicate its potential as a beneficial bacterium for agriculture applications, such as biocontrol of plant pathogens and promotion of plant growth.

CRediT authorship contribution statement

Xiaoyan Liang: Methodology, Investigation, Writing – original draft. Shumila Ishfaqa ： Writing – original draft. Yang Liu: Funding acquisition. M. Haissam Jijakli: Writing – review & editing. Xueping Zhou: Writing – review & editing. Xiuling Yang: Conceptualization, Writing – review & editing. Wei Guo: Conceptualization, Formal analysis, Methodology, Writing – review & editing, Supervision, Project administration, Funding acquisition.

Acknowledgments

This work was supported by the National Key Research and Development Program of China (2022YFE0139500, 2022YFD1400100), the National Natural Science Foundation of China (No. 32072377), Agricultural Science and Technology Innovation

656 Program of Institute of Food Science and Technology, Chinese Academy of
657 Agricultural Sciences (CAAS-ASTIP-G2022-IFST-01). We express our gratitude to
658 Dr. Hailei Wei from the Institute of Agricultural Resources and Regional Planning,
659 Chinese Academy of Agricultural Sciences, for providing valuable comments and
660 suggestions.

661 **Reference**

662 Abdel-Aziz, S.M., Abo Elsoud, M.M., Anise, A.A.H., 2017. Chapter 2 - Microbial
663 biosynthesis: a repertory of vital natural products, in: Grumezescu, A.M., Holban,
664 A.M. (Eds.), Food biosynthesis. Academic Press, New York, pp. 25-54.
665 Alikhan, N.F., Petty, N.K., Ben Zakour, N.L., Beatson, S.A., 2011. BLAST Ring Image
666 Generator (BRIG): simple prokaryote genome comparisons. BMC Genomics.
667 12(1), 402. https://doi.org/10.1186/1471-2164-12-402.
668 Borriss, R., Chen, X.H., Rueckert, C., Blom, J., Becker, A., Baumgarth, B., Fan, B.,
669 Pukall, R., Schumann, P., Spröer, C., Junge, H., Vater, J., Pühler, A., Klenk, H.P.,
670 2011. Relationship of *Bacillus amyloliquefaciens* clades associated with strains
671 DSM7^{T} and FZB42^{T}: a proposal for *Bacillus amyloliquefaciens* subsp.
672 *amyloliquefaciens* subsp. nov. and *Bacillus amyloliquefaciens* subsp. *plantarum*
673 subsp. nov. based on complete genome sequence comparisons. Int. J. Syst. Evol.
674 Micr. 61(8), 1786-1801. https://doi.org/10.1099/ijs.0.023267-0.
675 Cantalapiedra C.P., Hernández-Plaza A., Letunic I., Bork P., Huerta-Cepas J., 2021.
676 eggNOG-mapper v2: functional annotation, orthology assignments, and domain
677 prediction at the metagenomic scale. Mol. Biol. Evol. 38(12), 5825-5829.
678 https://doi.org/10.1093/molbev/msab293.
679 Chen C., Wu Y., Li J., Wang X., Zeng Z., Xu J., Liu Y., Feng J., Chen H., He Y., Xia R.,
680 2023. TBtools-II: A "one for all, all for one" bioinformatics platform for biological
681 big-data mining. Mol. Plant 16(11), 1733-1742.

Published in : Microbiological Research, vol. 285, August 2024
DOI: 10.1016/j.micres.2024.127745
Status : Postprint (Author's version)

https://doi.org/10.1016/j.molp.2023.09.010.

Chen, Q., Hu, H., Gao, M., Xu, J., Zhou, Y., Sun, J., 2011. Screening and identification of a nitrogen-fixing bacteria with 1-aminocyclopropane-1-carboxylate deaminase activity. J. Plant Nutr. Fertilizers 17(6), 1515-1521. https://doi.org/10.11674/zwyf.2011.1111.Chen, X.H., Vater, J., Piel, J., Franke, P., Scholz, R., Schneider, K., Koumoutsi, A., Hitzeroth, G., Grammel, N., Strittmatter, A.W., Gottschalk, G., Süssmuth, R.D., Borriss, R., 2006. Structural and functional characterization of three polyketide synthase gene clusters in *Bacillus amyloliquefaciens* FZB42. J. Bacteriol. 188(11), 4024-4036. https://doi.org/10.1128/JB.00052-06.

Chen, X.H., Koumoutsi, A., Scholz, R., Eisenreich, A., Schneider, K., Heinemeyer, I., Morgenstern, B., Voss, B., Hess, W.R., Reva, O., Junge, H., Voigt, B., Jungblut, P.R., Vater, J., Süssmuth, R., Liesegang, H., Strittmatter, A., Gottschalk, G., Borriss, R., 2007. Comparative analysis of the complete genome sequence of the plant growth-promoting bacterium *Bacillus amyloliquefaciens* FZB42. Nat. Biotechnol. 25(9), 1007-1014. https://doi.org/10.1038/nbt1325.

Chen Y., Yang H., Shen Z., Ye J., 2022. Whole-genome sequencing and potassium-solubilizing mechanism of *Bacillus aryabhattai* SK1-7. Front Microbiol. 12, 722379. https://doi.org/10.3389/fmicb.2021.722379.

Cheng, W., Yan, X., Xiao, J., Chen, Y., Chen, M., Jin, J., Bai, Y., Wang, Q., Liao, Z., Chen, Q., 2020. Isolation, identification, and whole genome sequence analysis of the alginate-degrading bacterium *Cobetia* sp. cqz5-12. Sci. Rep. 10(1), 10920. https://doi.org/10.1038/s41598-020-67921-7.

Chowdhury, S.P., Hartmann, A., Gao, X., Borriss, R., 2015. Biocontrol mechanism by root-associated *Bacillus amyloliquefaciens* FZB42 - a review. Front. Microbiol. 6, 780. https://doi.org/10.3389/fmicb.2015.00780.

Cochrane, S.A., Vederas, J.C., 2016. Lipopeptides from *Bacillus* and *Paenibacillus* spp.: a gold mine of antibiotic candidates. Med. Res. Rev. 36(1), 4-31.

https://doi.org/10.1002/med.21321.

Ding Y., Ma N., Haseeb H.A., Dai Z., Zhang J., Guo W., 2023. Genome-wide transcriptome analysis of toxigenic *Fusarium verticillioides* in response to variation of temperature and water activity on maize kernels. Int. J. Food Microbiol. 410, 110494. https://doi.org/10.1016/j.ijfoodmicro.2023.110494.

Dinolfo, M.I., Martínez, M., Castañares, E., Arata, A.F., 2022. *Fusarium* in maize during harvest and storage: a review of species involved, mycotoxins, and management strategies to reduce contamination. Eur. J. Plant Pathol. 26, 548. https://doi.org/10.3389/fmicb.2016.00548.

Dunlap, C.A., Kim, S.J., Kwon, S.W., Rooney, A.P., 2016. *Bacillus velezensis* is not a later heterotypic synonym of *Bacillus amyloliquefaciens*; *Bacillus methylotrophicus*, *Bacillus amyloliquefaciens* subsp. *plantarum* and '*Bacillus oryzicola*' are later heterotypic synonyms of *Bacillus velezensis* based on phylogenomics. Int. J. Syst. Evol. Micr. 66(3), 1212-1217. https://doi.org/10.1099/ijsem.0.000858.

Fan, B., Blom, J., Klenk, H.-P., Borriss, R., 2017. *Bacillus amyloliquefaciens*, *Bacillus velezensis*, and *Bacillus siamensis* form an "Operational Group *B. amyloliquefaciens*" within the *B. subtilis* species complex. Front. Microbiol. 8, 22. https://doi.org/10.3389/fmicb.2017.00022.

Fierro-Coronado, R.A., Quiroz-Figueroa, F.R., García-Pérez, L.M., Ramírez-Chávez, E., Molina-Torres, J., Maldonado-Mendoza, I.E., 2014. IAA-producing rhizobacteria from chickpea (*Cicer arietinum* L.) induce changes in root architecture and increase root biomass. Can. J. Microbiol. 60(10), 639-648. https://doi.org/10.1139/cjm-2014-0399.

Gai, X., Dong, H., Wang, S., Liu, B., Zhang, Z., Li, X., Gao, Z., 2018. Infection cycle of maize stalk rot and ear rot caused by *Fusarium verticillioides*. PLoS One. 13(7), e0201588. https://doi.org/10.1371/journal.pone.0201588.

González-Estrada, R.R., Blancas-Benitez, F.J., Aguirre-Güitrón, L., Hernandez-

738 Montiel, L.G., Moreno-Hernández, C., Cortés-Rivera, H.J., Herrera-González,
739 J.A., Rayón-Díaz, E., Velázquez-Estrada, R.M., Santoyo-González, M.A.,
740 Gutierrez-Martinez, P., 2021. Chapter 5 - Alternative management technologies
741 for postharvest disease control, in: Galanakis, C.M. (Eds.), Food losses,
742 sustainable postharvest and food technologies. Academic Press, New York, pp.
743 153-190.
744 Grigoreva A., Andreeva J., Bikmetov D., Rusanova A., Serebryakova M., Garcia A.H.,
745 Slonova D., Nair S.K., Lippens G., Severinov K., Dubiley S., 2021. Identification
746 and characterization of andalusicin: N-terminally dimethylated class III lantibiotic
747 from *Bacillus thuringiensis* sv. *andalousiensis*. iScience 24(5), 102480.
748 https://doi.org/10.1016/j.isci.2021.102480.
749 Gundlach J., Herzberg C., Kaever V., Gunka K., Hoffmann T., Weiß M., Gibhardt J.,
750 Thürmer A., Hertel D., Daniel R., Bremer E., Commichau F.M., Stülke J., 2017.
751 Control of potassium homeostasis is an essential function of the second messenger
752 cyclic di-AMP in *Bacillus subtilis*. Sci. Signal. 10(475), eaal3011.
753 https://doi.org/10.1126/scisignal.aal3011.
754 Gupta, K., Dubey, N.K., Singh, S.P., Kheni, J.K., Gupta, S., Varshney, A., 2021a. Plant
755 Growth-Promoting Rhizobacteria (PGPR): Current and future prospects for crop
756 improvement, in: Yadav, A.N., Singh, J., Singh, C., Yadav, N. (Eds.), Current
757 trends in microbial biotechnology for sustainable agriculture. Springer, Singapore,
758 pp. 203-226.
759 Gupta, M., Topgyal, T., Zahoor, A., Gupta, S., 2021b. Chapter 15 - Rhizobium: Eco-
760 friendly microbes for global food security, in: Kumar, A., Droby, S. (Eds.),
761 Microbial management of plant stresses. Woodhead Publishing, Cambridgeshire
762 pp. 221-233.
763 Harwood, C.R., Mouillon, J.-M., Pohl, S., Arnau, J., 2018. Secondary metabolite
764 production and the safety of industrially important members of the *Bacillus*
765 *subtilis* group. FEMS Microbiol. Rev. 42(6), 721-738.

https://doi.org/10.1093/femsre/fuy028.

Haskett, T.L., Tkacz, A., Poole, P.S., 2020. Engineering rhizobacteria for sustainable agriculture. ISME J. 15, 949–964. https://doi.org/10.1038/s41396-020-00835-4.

Heifetz, C.L., Fisher, M.W., Chodubski, J.A., DeCarlo, M.O., 1972. Butirosin, a new aminoglycosidic antibiotic complex: antibacterial activity *in vitro* and in mice. Antimicrob. Agents Ch. 2(2), 89-94. https://doi.org/10.1128/AAC.2.2.89.

Keswani, C., Singh, S.P., Cueto, L. García-Estrada C., Mezaache-Aichour S., Glare T.R., Borriss R., Singh S.P., Blázquez M.A., Sansinenea E., 2020. Auxins of microbial origin and their use in agriculture. Appl. Microbiol. Biotechnol. 104, 8549–8565. https://doi.org/10.1007/s00253-020-10890-8

Kloepper, J.W., Leong, J., Teintze, M., Schroth, M.N., 1980. Enhanced plant growth by siderophores produced by plant growth-promoting rhizobacteria. Nature 286(5776), 885-886. https://doi.org/10.1038/286885a0.

Kujawa, M., 1994. Some naturally occurring substances: Food items and constituents, heterocyclic aromatic amines and mycotoxins, in: International Agency for Research on Cancer (Eds.), IARC monographs on the evaluation of carcinogenic risks to humans. World Health Organization, Lyon, pp: 351-351.

Li, B., Li, Q., Xu, Z., Zhang, N., Shen, Q., Zhang, R., 2014. Responses of beneficial *Bacillus amyloliquefaciens* SQR9 to different soilborne fungal pathogens through the alteration of antifungal compounds production. Front. Microbiol. 5, 636. https://doi.org/10.3389/fmicb.2014.00636.

Li, L., Qu, Q., Cao, Z., Guo, Z., Jia, H., Liu, N., Wang, Y., Dong, J., 2019. The relationship analysis on corn stalk rot and ear rot according to *Fusarium* species and fumonisin contamination in kernels. Toxins, 11, 320. https://doi.org/10.3390/toxins11060320.

Liang, X., Zhang, X., Haseeb, H.A., Tang, T., Shan, J., Yin, B., Guo, W., 2022. Development and evaluation of a novel visual and rapid detection assay for toxigenic *Fusarium graminearum* in maize based on recombinase polymerase

amplification and lateral flow analysis. Int. J. Food Microbiol. 372, 109682. https://doi.org/10.1016/j.ijfoodmicro.2022.109682.

Lin, F., Xue, Y., Huang, Z., Jiang, M., Lu, F., Bie, X., Miao, S., Lu, Z., 2019. Bacillomycin D inhibits growth of *Rhizopus stolonifer* and induces defense-related mechanism in cherry tomato. Appl. Microbiol. Biot. 103(18), 7663-7674. https://doi.org/10.1007/s00253-019-09991-w.

Ma, R., Zhang, A., Hui, X., Dai M., Wang W., Zhu, B., 2013. Screening, identification and sporulation conditions optimization of NX-11 strain having the ability of solubilizing phosphorus and potassium. Acta Agriculturae Boreali-Sinica 28(2), 202-208. https://doi.org/10.3969/j.issn.1000-7091.2013.02.036

Madigan, M.T., Imhoff, J.F., 2001. Phylum BXIII. Firmicutes, in: Boone, D.R., Castenholz, R.W., Garrity, G.M. (Eds), Bergey's manual of systematic bacteriology. Springer, New York.

Mongkolthanaruk, W., 2012. Classification of *Bacillus* beneficial substances related to plants, humans and animals. J. Microbiol. Biotechn. 22, 1597-1604. https://doi.org/10.4014/jmb.1204.04013

Moreno-Letelier A., Olmedo G., Eguiarte L.E., Martinez-Castilla L., Souza V., 2011. Parallel evolution and horizontal gene transfer of the pst operon in *Firmicutes* from oligotrophic environments. Int. J. Evol. Biol. 2011, 781642. https://doi.org/10.4061/2011/781642.

Nautiyal, C.S., 1999. An efficient microbiological growth medium for screening phosphate solubilizing microorganisms. FEMS Microbiol. Lett. 170(1), 265-270. https://doi.org/10.1111/j.1574-6968.1999.tb13383.x.

Ongena, M., Jourdan, E., Adam, A., Paquot, M., Brans, A., Joris, B., Arpigny, J.L., Thonart, P., 2007. Surfactin and fengycin lipopeptides of *Bacillus subtilis* as elicitors of induced systemic resistance in plants. Environ. Microbiol. 9(4), 1084-1090. https://doi.org/10.1111/j.1462-2920.2006.01202.x

Pereira, P.C.G., Parente, C.E.T., Carvalho, G.O., Torres, J.P.M., Meire, R.O., Dorneles,

P.R., Malm, O., 2021. A review on pesticides in flower production: A push to reduce human exposure and environmental contamination. Environ. Pollut. 289, 117817. https://doi.org/10.1016/j.envpol.2021.117817.

Ruiz-García, C., Béjar, V., Martínez-Checa, F., Llamas, I., Quesada, E., 2005. *Bacillus velezensis* sp. nov., a surfactant-producing bacterium isolated from the river Vélez in Málaga, southern Spain. Int. J. Syst. Evol. Micr. 55(1), 191-195. https://doi.org/10.1099/ijs.0.63310-0.

Ryu M.H., Zhang J., Toth T., Khokhani D., Geddes B.A., Mus F., Garcia-Costas A., Peters J.W., Poole P.S., Ané J.M., Voigt C.A., 2020. Control of nitrogen fixation in bacteria that associate with cereals. Nat. Microbiol. 5(2), 314-330. https://doi.org/10.1038/s41564-019-0631-2

Savary, S., Willocquet, L., Pethybridge, S.J., Esker, P., McRoberts, N., Nelson, A., 2019. The global burden of pathogens and pests on major food crops. Nat. Ecol. Evol. 3(3), 430-439. https://doi.org/10.1038/s41559-018-0793-y.

Sritongon N., Boonlue S., Mongkolthanaruk W., Jogloy S., Riddech N., 2023. The combination of multiple plant growth promotion and hydrolytic enzyme producing rhizobacteria and their effect on Jerusalem artichoke growth improvement. Sci. Rep. 13(1), 5917. https://doi.org/10.1038/s41598-023-33099-x.

Tabassum, B., Khan, A., Tariq, M., Ramzan, M., Iqbal-Khan, M.S., Shahid, N., Aaliya, K., 2017. Bottlenecks in commercialisation and future prospects of PGPR. Appl. Soil Ecol. 121, 102-117. https://doi.org/10.1016/j.apsoil.2017.09.030.

Tanaka, H., Watanabe, T., 1995. Glucanases and chitinases of *Bacillus circulans* WL-12. J. Ind. Microbiol. Biot. 14(6), 478-483. https://doi.org/10.1007/BF01573962.

Torres P., Altier N., Beyhaut E., Fresia P., Garaycochea S., Abreo E., 2023. Phenotypic, genomic and in planta characterization of *Bacillus sensu lato* for their phosphorus biofertilization and plant growth promotion features in soybean. Microbiol Res. 280, 127566. https://doi.org/10.1016/j.micres.2023.

Tunsagool, P., Jutidamrongphan, W., Phaonakrop, N., Jaresitthikunchai, J., Roytrakul,

S., Leelasuphakul, W., 2019. Insights into stress responses in mandarins triggered by *Bacillus subtilis* cyclic lipopeptides and exogenous plant hormones upon *Penicillium digitatum* infection. Plant Cell Rep. 38(5), 559-575. https://doi.org/10.1007/s00299-019-02386-1.

Wang, F., Xiao, J., Zhang, Y., Li, R., Liu, L., Deng, J., 2021. Biocontrol ability and action mechanism of *Bacillus halotolerans* against *Botrytis cinerea* causing grey mould in postharvest strawberry fruit. Postharvest Biol. Tec. 174, 111456. https://doi.org/10.1016/j.postharvbio.2020.111456

Wang L., Zhang L., Liu Z., Zhao D., Liu X., Zhang B., Xie J., Hong Y., Li P., Chen S., Dixon R., Li J., 2013. A minimal nitrogen fixation gene cluster from *Paenibacillus* sp. WLY78 enables expression of active nitrogenase in *Escherichia coli*. PLoS Genet. 9(10), e1003865. https://doi.org/10.1371/journal.pgen.1003865.

Wang, L., Lee, F., Tai, C., Kasai, H., 2007. Comparison of *gyrB* gene sequences, *16S rRNA* gene sequences and DNA–DNA hybridization in the *Bacillus subtilis* group. Int. J. Syst. Evol. Micr. 57(8), 1846-1850. https://doi.org/10.1099/ijs.0.64685-0.

Wang, L., Lee, F., Tai, C., Kuo, H., 2008. *Bacillus velezensis* is a later heterotypic synonym of *Bacillus amyloliquefaciens.* Int. J. Syst. Evol. Micr. 58(3), 671-675. https://doi.org/10.1099/ijs.0.65191-0.

Wu, G., Liu, Y., Xu, Y., Zhang, G., Shen, Q., Zhang, R., 2018. Exploring elicitors of the beneficial rhizobacterium *Bacillus amyloliquefaciens* SQR9 to induce plant systemic resistance and their interactions with plant signaling pathways. Mol. Plant Microbe In. 31(5), 560-567. https://doi.org/10.1094/MPMI-11-17-0273-R.

Xu, L., Dong, Z., Fang, L., Luo, Y., Wei, Z., Guo, H., Zhang, G., Gu, Y.Q., Coleman-Derr, D., Xia, Q., Wang, Y., 2019. OrthoVenn2: a web server for whole-genome comparison and annotation of orthologous clusters across multiple species. Nucleic Acids Res. 47(1), 52-58. https://doi.org/10.1093/nar/gkz333.

Xu, Z., Shao, J., Li, B., Yan, X., Shen, Q., Zhang, R., 2013. Contribution of bacillomycin D in *Bacillus amyloliquefaciens* SQR9 to antifungal activity and

Published in : Microbiological Research, vol. 285, August 2024
DOI: 10.1016/j.micres.2024.127745
Status : Postprint (Author's version)

biofilm formation. Appl. Environ. Microb. 79(3), 808-815. https://doi.org/10.1128/AEM.02645-12.

Yamamoto, S., Harayama, S., 1995. PCR amplification and direct sequencing of *gyrB* genes with universal primers and their application to the detection and taxonomic analysis of *Pseudomonas putida* strains. Appl. Environ. Microbiol. 61(3), 1104-1109. https://doi.org/10.1128/aem.61.3.1104-1109.1995.

Yu Y., Yan F., Chen Y., Jin C., Guo J.H., Chai Y., 2016. Poly-γ-glutamic acids contribute to biofilm formation and plant root colonization in selected environmental isolates of *Bacillus subtilis*. Front. Microbiol. 7, 1811. https://doi.org/10.3389/fmicb.2016.01811.

Zawadzka A.M., Kim Y., Maltseva N., Nichiporuk R., Fan Y., Joachimiak A., Raymond K.N., 2009. Characterization of a *Bacillus subtilis* transporter for petrobactin, an anthrax stealth siderophore. Proc. Natl. Acad. Sci. U. S. A. 106(51), 21854-21859. https://doi.org/10.1073/pnas.0904793106.

Zhang, F., Tang, T., Li, F. Guo W., 2023. Characterization of mating type, spore killing, and pathogenicity of *Fusarium verticillioides* populations from maize in China. Phytopathol. Res. 5, 40. https://doi.org/10.1186/s42483-023-00195-9

Zhang, J., Cui, W., Haseeb A.H., Guo, W., 2020. VdNop12, containing two tandem RRM domains, is a crucial factor for pathogenicity and cold adaption in *Verticillium dahliae*. Environ. Microbiol. 22(12), 5387-5401. https://doi.org/10.1111/1462-2920.15268.

Zhang, N., Yang, D., Wang, D., Miao, Y., Shao, J., Zhou, X., Xu, Z., Li, Q., Feng, H., Li, S., Shen, Q., Zhang, R., 2015. Whole transcriptomic analysis of the plant-beneficial rhizobacterium *Bacillus amyloliquefaciens* SQR9 during enhanced biofilm formation regulated by maize root exudates. BMC Genomics 16(1), 685. https://doi.org/10.1186/s12864-015-1825-5.

Zhu, H., Feng, Z., Li, Z., Shi, Y., Zhao, L., Yang, J., 2013. Characterization of two fungal isolates from cotton and evaluation of their potential for biocontrol of

Published in : Microbiological Research, vol. 285, August 2024
DOI: 10.1016/j.micres.2024.127745
Status : Postprint (Author's version)

906 Verticillium wilt of cotton. J. Phytopathol. 161(2), 70-77.
907 https://doi.org/10.1111/jph.12027.
908

Published in : Microbiological Research, vol. 285, August 2024
DOI: 10.1016/j.micres.2024.127745
Status : Postprint (Author's version)

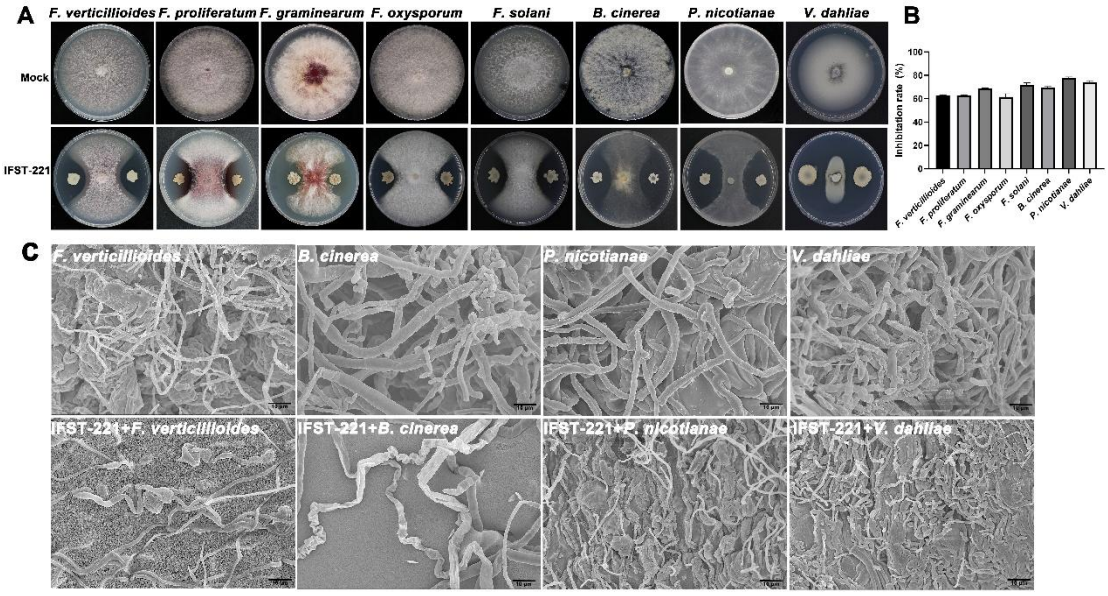

Figure 1 Antagonistic activity of strain IFST-221 against eight different phytopathogens. (A) The antagonistic spectrum of strain IFST-221 *in vitro*. *Fusarium verticillioides*, *F. proliferatum*, *F. graminearum*, *F. oxysporum*, *F. solani*, *Botrytis cinerea*, *Phytophthora nicotianae*, and *Verticillium dahliae* were used to test the antimicrobial activity. (B) Inhibition rates of strain IFST-221 against eight phytopathogens. Error bars represent standard errors. (C) Scanning electron microscopy images showing the morphological changes of *F. verticillioides*, *B. cinerea*, *P. nicotianae*, and *V. dahliae* after co-incubation with IFST-221.

Published in : Microbiological Research, vol. 285, August 2024
DOI: 10.1016/j.micres.2024.127745
Status : Postprint (Author's version)

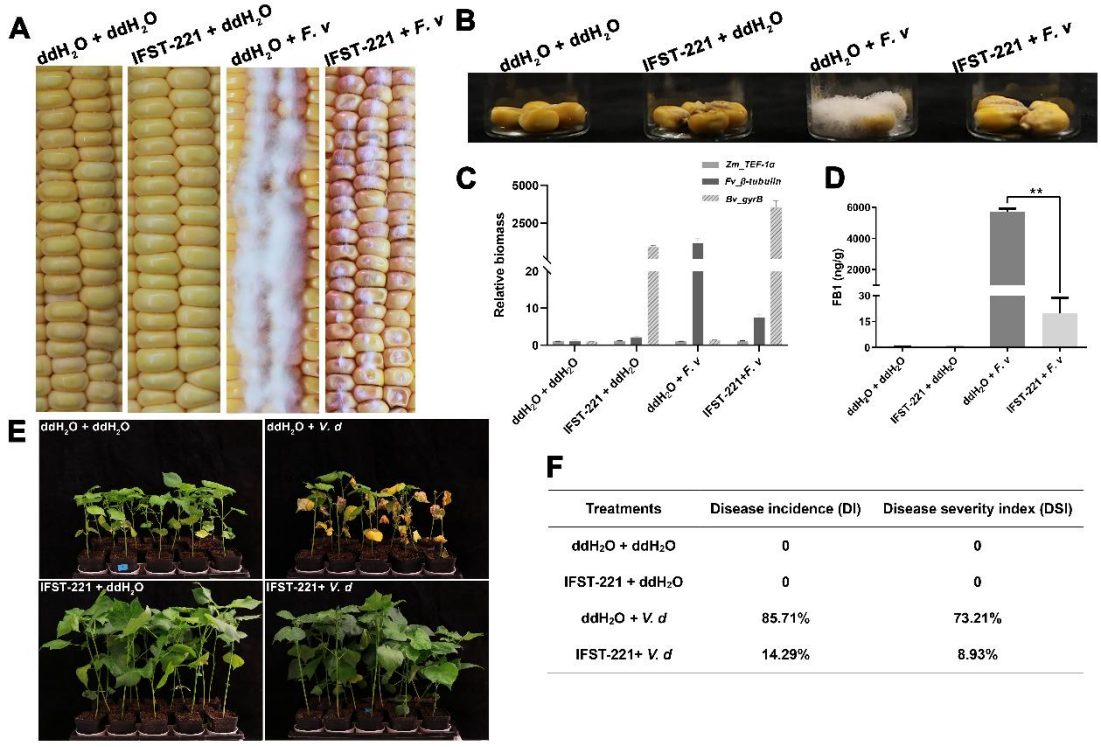

F

Treatments	Disease incidence (DI)	Disease severity index (DSI)
ddH_2O + ddH_2O	0	0
IFST-221 + ddH_2O	0	0
ddH_2O + *V. d*	85.71%	73.21%
IFST-221+ *V. d*	14.29%	8.93%

Figure 2 The inhibitory effects of IFST-221 against ear rot of maize and Verticillium wilt of cotton plants. (A and B) Effect of IFST-221 on the development of *F. verticillioides* in maize ears and kernels, respectively. Maize ears and kernels pretreated with ddH_2O or IFST-221 were then inoculated with *F. verticillioides* or ddH_2O. Representative photos were captured at 5 days post-inoculation. (C) Quantitative PCR (qPCR) analysis of the fungal and bacterial biomass on maize kernels. Error bars represented standard errors. (D) HPLC-MS analysis of the level of fumonisin B_1 (FB_1) in maize kernels under different treatments. Double asterisks (**) indicate $p < 0.01$ determined by Student's *t*-test. (E) Assessment of the efficacy of IFST-221 in controlling Verticillium wilt of cotton plants. (F) The disease incidence (DI) and disease severity index (DSI) of Verticillium wilt under different treatments.

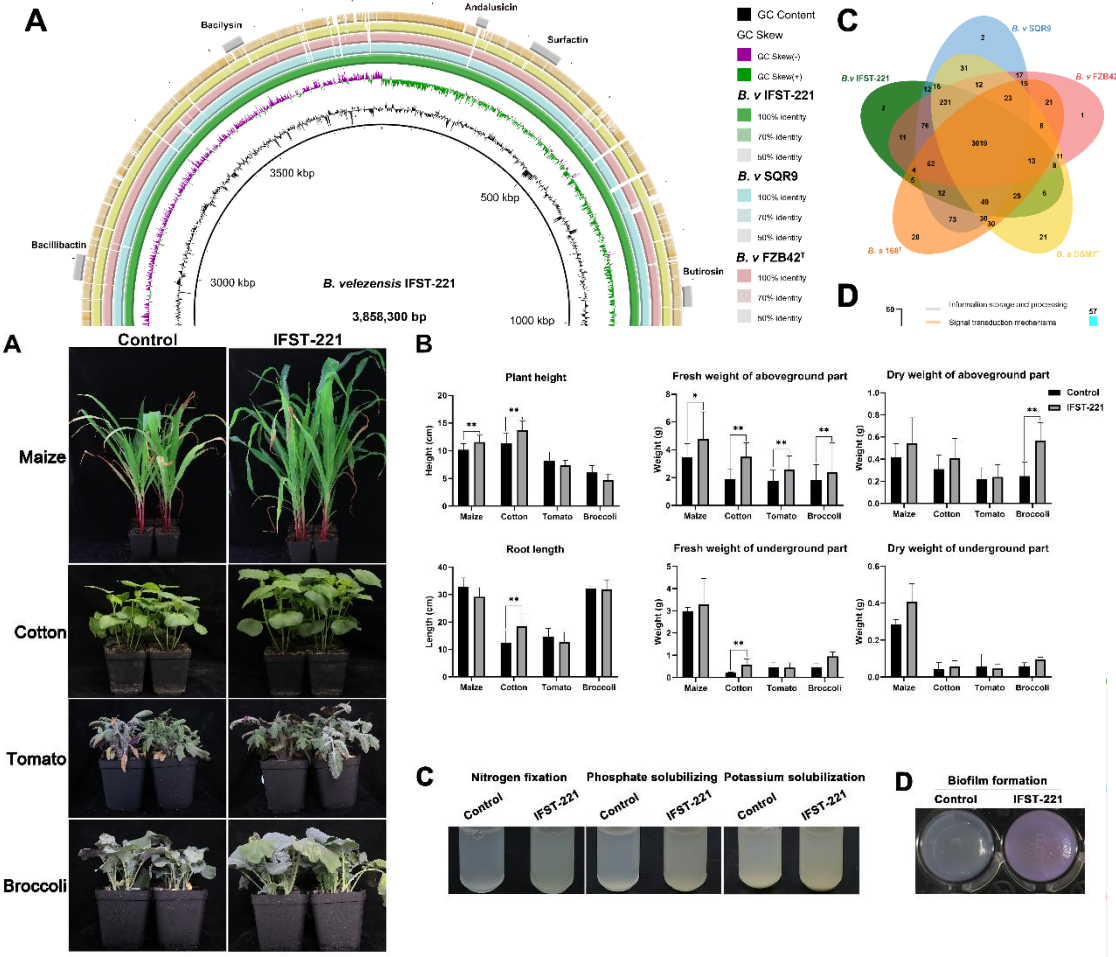

Figure 3 The plant growth-promoting activity of IFST-221. (A) Effect of IFST-221 on the growth of maize, cotton, tomato, and broccoli seedlings. Photos were captured at 30 days post inoculation (dpi). Seedlings exposed to the Fertilizer "HUABAO No. 2" were used as controls. (B) Measurements of plant height, fresh and dry weight of the aboveground, root length, and fresh and dry weight of the underground part of maize, cotton, tomato, and broccoli seedlings treated with IFST-221 or HUABAO Fertilizer "HUABAO No. 2" at 30 dpi. Error bars indicate standard errors. A single asterisk (*) indicates a significant difference of $p < 0.05$. Double asterisks (**) indicate a highly significant difference of $p < 0.01$. (C) Ability of IFST-221 to fix nitrogen and to solubilize phosphate and potassium *in vitro*. The IFST-221 was cultivated under different cultures, with ddH_2O serving as the control. (D) Biofilm formation of IFST-221 stained with crystal violet.

Published in : Microbiological Research, vol. 285, August 2024
DOI: 10.1016/j.micres.2024.127745
Status : Postprint (Author's version)

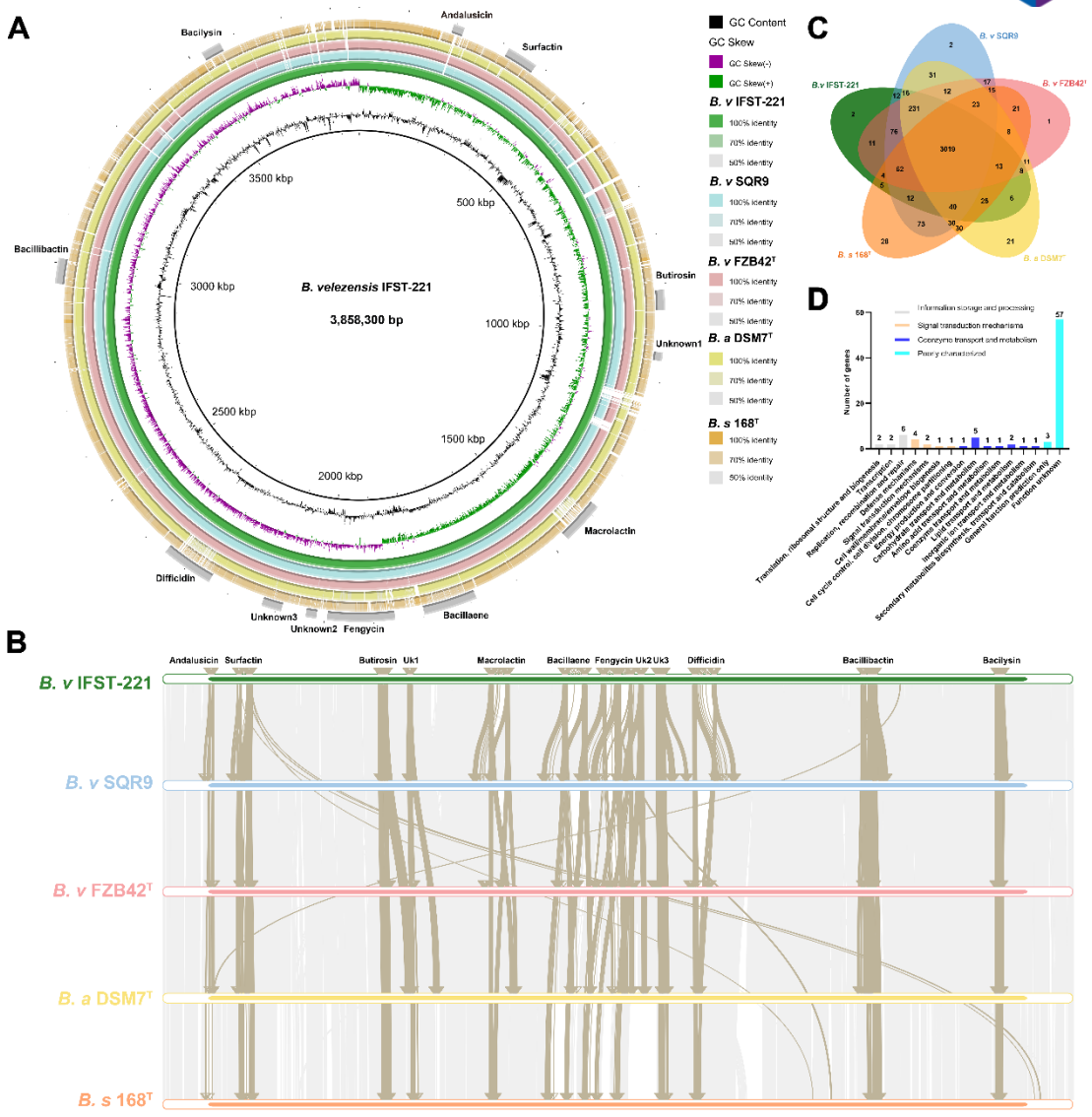

Figure 4 Comparative genomic analysis of *Bacillus velezensis* IFST-221 with *B. velezensis* SQR9 and FZB42^T, *B. amyloliquefaciens* DSM7^T, and *B. subtilis* 168^T. (A) The comparative genomic circle map was constructed using BRIG v0.95. The features are as follows (from center to outside): circle 1 is genome size; circle 2 is GC Content; circle 3 is GC Skew; circles 4 to 8 are the comparative genomic maps of *B. velezensis* IFST-221, SQR9, FZB42^T, *B. amyloliquefaciens* DSM7^T, and *B. subtilis* 168^T, respectively; the outermost circle indicates the positions of gene clusters of predicted secondary metabolites. (B) Synteny analysis of five strains and IFST-221 genome was used as the reference genome. Grey indicated a sequence with synteny and the genes of secondary metabolites were shown in brown. (C) Venn diagram showing the number of unique, accessory, and core genes shared by *B. velezensis* IFST-221, SQR9, FZB42^T,

Published in : Microbiological Research, vol. 285, August 2024
DOI: 10.1016/j.micres.2024.127745
Status : Postprint (Author's version)

B. amyloliquefaciens DSM7^T, and *B. subtilis* 168^T. The core and accessory genes are those located at the intersection of the five circles. The number of unique genes of each species is shown in each corresponding circle. Annotation was performed using OrthoVenn2. (D) Classification of annotated singleton (genes for which no orthologs could be found in other species) functions in the COG (Clusters of Orthologous Groups) for *B. velezensis* IFST-221.

Published in : Microbiological Research, vol. 285, August 2024
DOI: 10.1016/j.micres.2024.127745
Status : Postprint (Author's version)

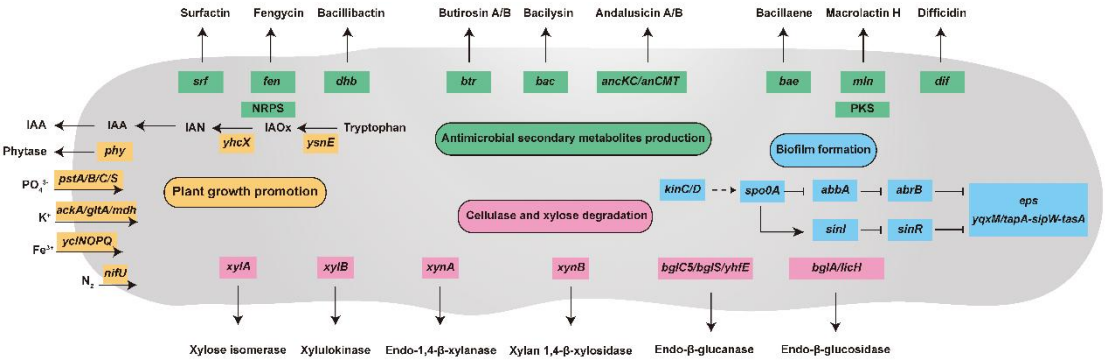

Figure 5 The key genes potentially participating in antimicrobial secondary metabolites (green color), plant growth promotion (yellow color), cellulase and xylose degradation (pink color), and biofilm formation (blue color) in the IFST-221 genome.

Published in : Microbiological Research, vol. 285, August 2024
DOI: 10.1016/j.micres.2024.127745
Status : Postprint (Author's version)

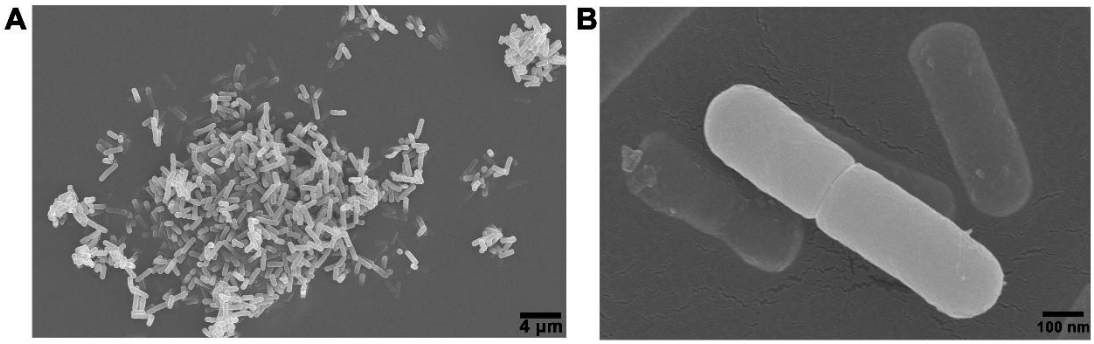

966 **Figure S1** Scanning electron microscopy of the morphology of IFST-221 after
967 incubation in LB broth at 37 °C for 12 hours. (A) Scale bar, 4 µm (B) Scale bar, 100
968 nm.

969

Published in : Microbiological Research, vol. 285, August 2024
DOI: 10.1016/j.micres.2024.127745
Status : Postprint (Author's version)

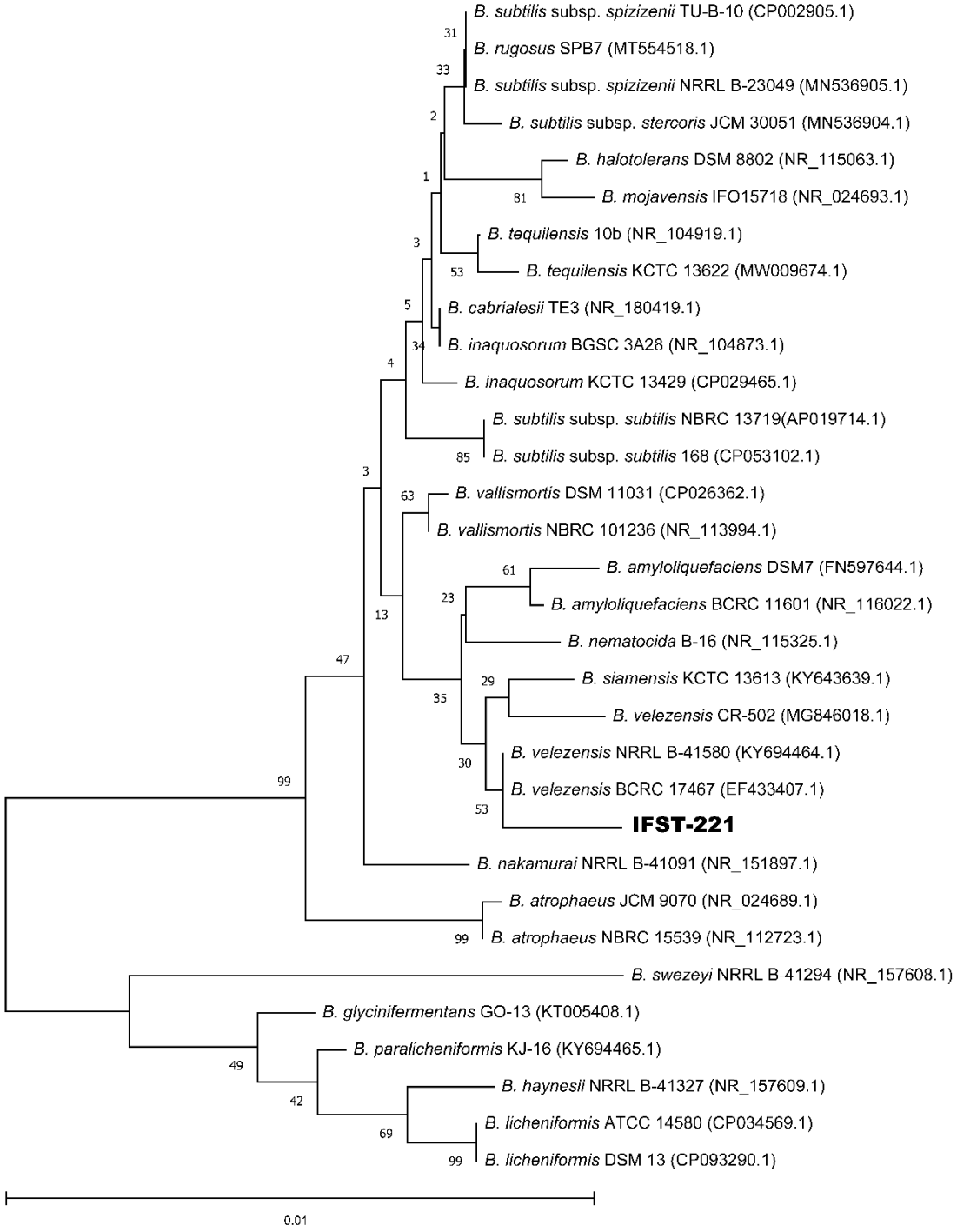

Figure S2 A neighbor-joining phylogenetic tree was constructed using the *16S rDNA* gene sequence of IFST-221 and other closely related *Bacillus* species. The significance of each branch is indicated by a bootstrap value (%) calculated for 1000 subsets. Genbank accession numbers are given in parentheses. Bar, 0.01 substitutions per nucleotide position.

Published in : Microbiological Research, vol. 285, August 2024
DOI: 10.1016/j.micres.2024.127745
Status : Postprint (Author's version)

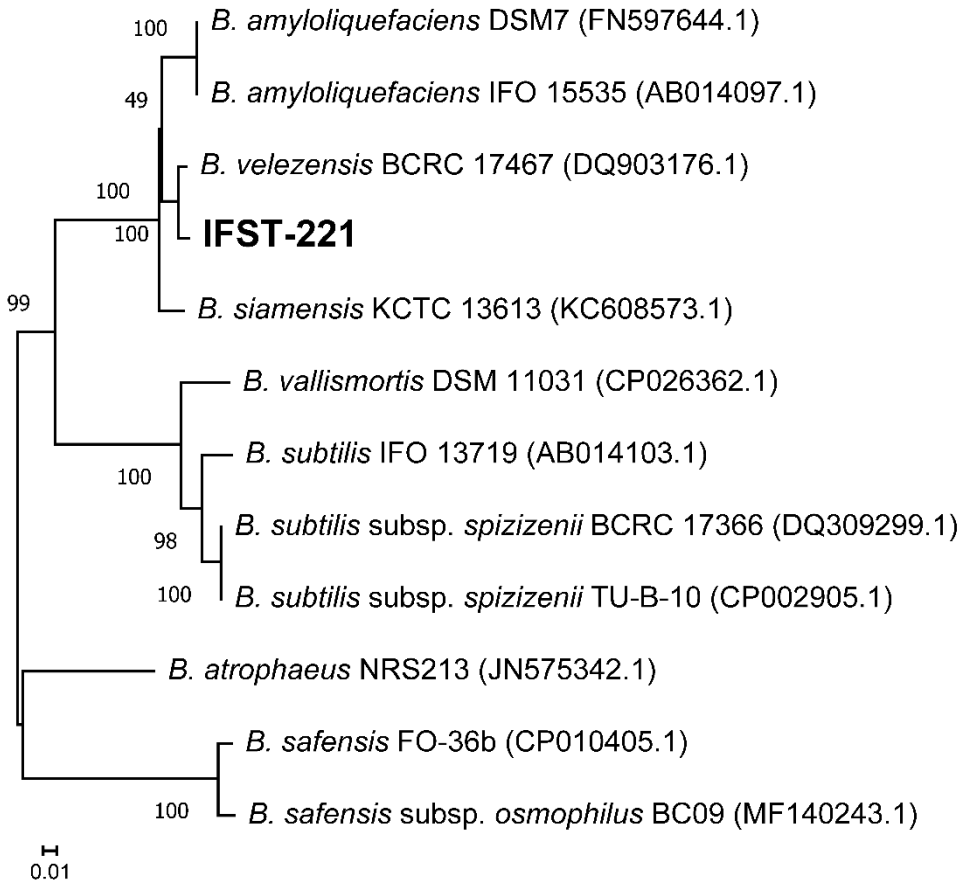

Figure S3 A phylogenetic tree of IFST-221 constructed using the nucleotide sequences of *gyrB* (subunit B protein of DNA gyrase) based on the neighbor-joining method. The significance of each branch is indicated by a bootstrap value (%) calculated for 1000 subsets. Genbank accession numbers are given in parentheses. Bar represents 0.01 substitutions per nucleotide position.

Published in : Microbiological Research, vol. 285, August 2024
DOI: 10.1016/j.micres.2024.127745
Status : Postprint (Author's version)

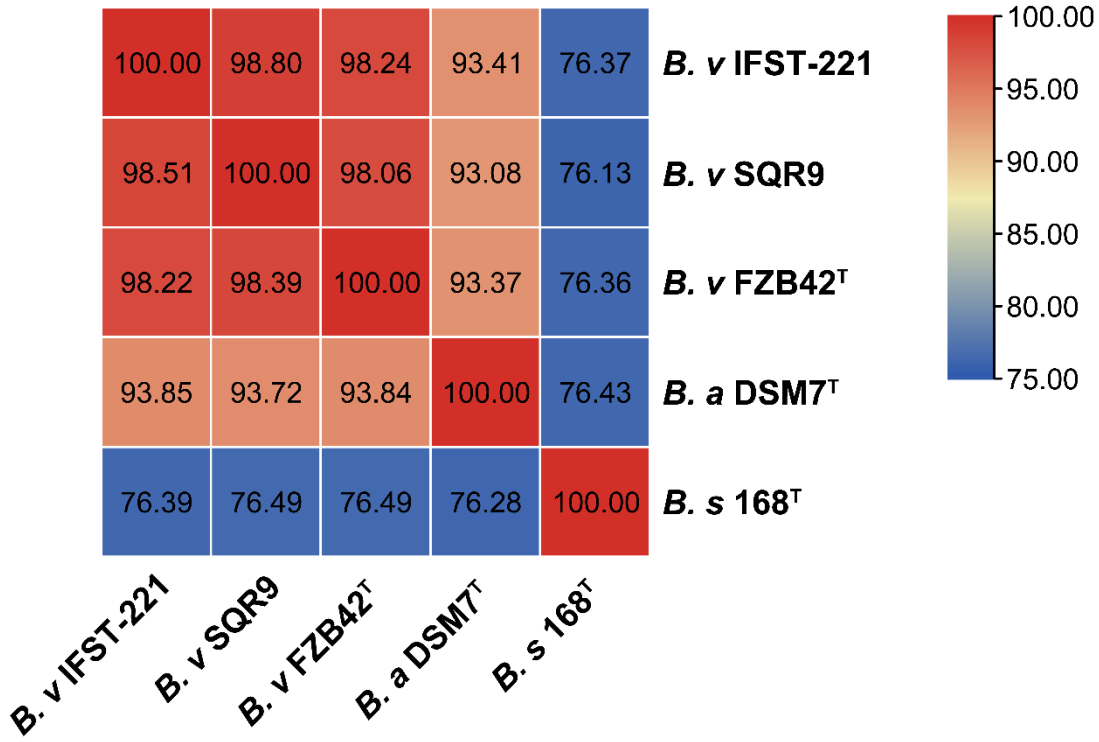

Figure S4 Heatmap of the Average Nucleotide Identity (ANI) values for the genomes of five *Bacillus* strains, including *B. velezensis* IFST-221, SQR9, FZB42^T, *B. amyloliquefaciens* DSM7^T, and *B. subtilis* 168^T.

Published in : Microbiological Research, vol. 285, August 2024
DOI: 10.1016/j.micres.2024.127745
Status : Postprint (Author's version)

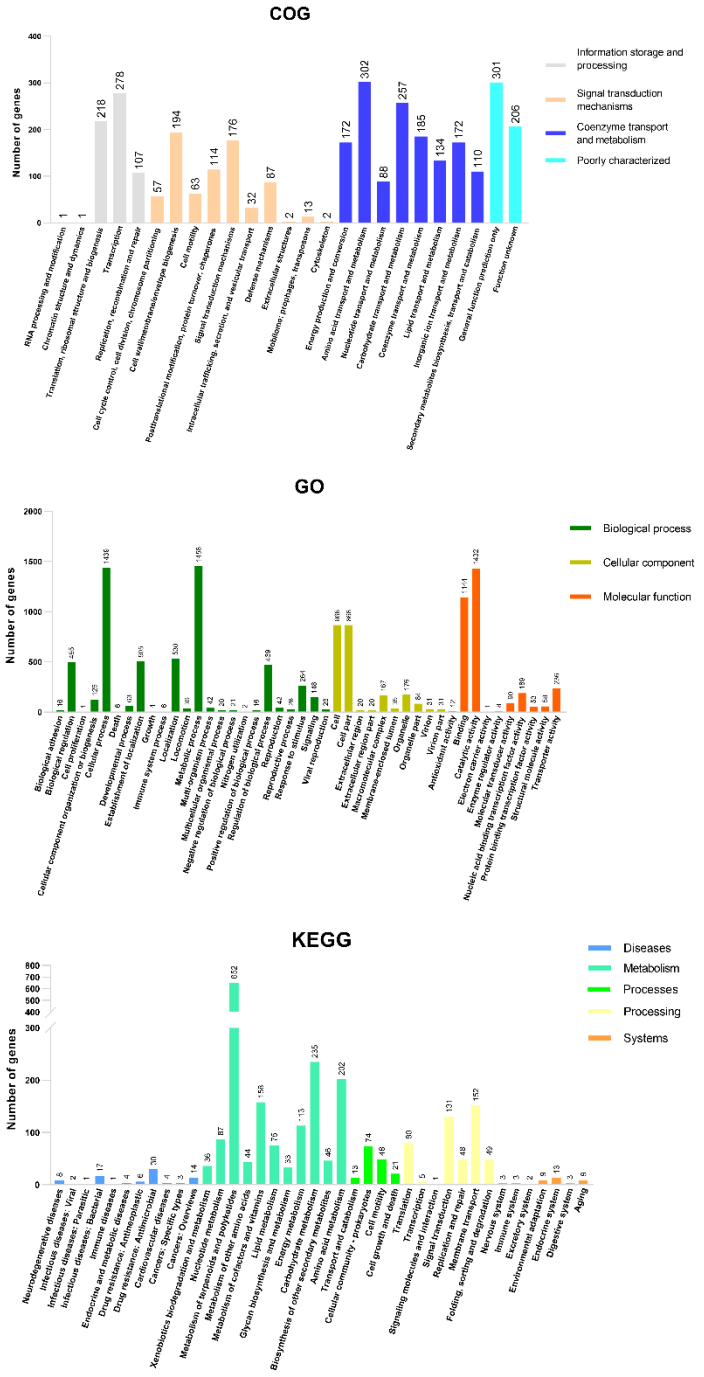

Figure S5 Classification of annotated gene functions in the (A) COG (Clusters of Orthologous Groups), (B) GO (Gene Ontology), and (C) KEGG (Kyoto Encyclopedia of Genes and Genomes) for the whole genome of *B. velezensis* IFST-221.

Published in : Microbiological Research, vol. 285, August 2024
DOI: 10.1016/j.micres.2024.127745
Status : Postprint (Author's version)

Table 1 Genomic comparison between *B. velezensis* IFST-221, *B. velezensis* SQR9, *B. velezensis* FZB42^T, *B. amyloliquefaciens* DSM7^T, and *B. subtilis* 168^T.

Features	*B. velezensis* IFST-221	*B. velezensis* SQR9	*B. velezensis* FZB42 ^{T}	*B. amyloliquefaciens* DSM7^T	*B. subtilis* 168^T
Genome size (bp)	3,858,300	4,117,023	3,918,600	3,980,200	4,215,606
GC content (mol%)	46.71	46.1	46.5	46.1	43.5
Protein-coding sequences	3659	4078	3693	3921	4237
Average CDS size (bp)	875	916	933	888	895
Percent of coding region	90.06	89.0	88.0	87.0	87.2
Numbers of tRNAs	86	72	88	93	86
Ribosomal RNA operons	9	7	10	10	10

Note: The genomic information of IFST-221 was predicted by GeneMarkS software (http://topaz.gatech.edu/). And the genomic information of *B. velezensis* SQR9, *B. velezensis* FZB42^T, *B. amyloliquefaciens* DSM7^T, and *B. subtilis* 168^T were obtained from Chen et al. (2007) and Zhang et al. (2015)

Published in : Microbiological Research, vol. 285, August 2024
DOI: 10.1016/j.micres.2024.127745
Status : Postprint (Author's version)

Table 2 Comparison of predicted and known secondary metabolites between *B. velezensis* IFST-221, *B. velezensis* SQR9, *B. velezensis* FZB42^T, *B. amyloliquefaciens* DSM7^T, and *B. subtilis* 168^T.

Cluster	***B. velezensis* IFST-221**	***B. velezensis* SQR9**	***B. velezensis* FZB42^T**	***B. amyloliquefaciens* DSM 7^T**	***B. subtilis* 168^T**
1	**Surfactin**	Surfactin	Surfactin	Surfactin	Surfactin
2	**Fengycin**	Fengycin	Fengycin	Fengycin	Fengycin
3	**Bacillibactin**	Bacillibactin	Bacillibactin	Bacillibactin	Bacillibactin
4	**Macrolactin H**	Macrolactin H	Macrolactin H	Unknown	Subtilosin A
5	**Difficidin**	Difficidin	Difficidin	Unknown	Sporulation killing factor
6	**Bacillaene**	Bacillaene	Bacillaene	Bacillaene	Bacillaene
7	**Bacilysin**	Bacilysin	Bacilysin	Bacilysin	Bacilysin
8	**Butirosin A/B**	Butirosin A/B	Butirosin A/B	Butirosin A/B	Sublancin 168
9	**Andalusicin A/B**	Dumulmycin / Shuangdaolide A/B/C/D	Plantazolicin	Unknown 1	1-carbapen-2-em-3-carboxylic acid
10	**Unknown 1**	Unknown 1	Bacillothiazol A/B/C/D/E/F/G//H/I/J/K/L/M/N	Unknown 2	Pulcherriminic acid
11	**Unknown 2**	Unknown 2	Unknown 1	Unknown 3	Thailanstatin A
12	**Unknown 3**	Unknown 3	Unknown 2	-	Unknown 1
13	-	-	Unknown 3	-	Unknown 2
14	-	-	-	-	Unknown 3

-, Not applicable

Published in : Microbiological Research, vol. 285, August 2024
DOI: 10.1016/j.micres.2024.127745
Status : Postprint (Author's version)

Table S1 Physiological and biochemical results of strain IFST-221.

Tests	IFST-221	Tests	IFST-221
Gram stain	+	Dextrose	+
Growing in pH 5.7	+	L-Arabinose	+
Growing in pH 6.8	+	D-xylose	+
Growing at 15 °C	+	Mannitol	+
Growing at 40 °C	+	Starch	+
Growing in 10 % NaCl	-	Methyl red (MR) test	+
Growing in 7 % NaCl	+	Voges-proskauer (VP) tests	+
Growing in 5 % NaCl	+	Casein hydrolysis	+
Growing in 2 % NaCl	+	Citrate utilization test	+
ONPG production test	+		

"+" represents "Positive" and "-" represents "Negative".

Published in : Microbiological Research, vol. 285, August 2024
DOI: 10.1016/j.micres.2024.127745
Status : Postprint (Author's version)

Table S2. Primers used in this study.

Name	Sequences (5′→3′)	Purpose
27F	AGAGTTTGATCCTGGCTCAG	Partial 16S rDNA gene amplification
1492R	TACGGCTACCTTGTTACGACTT	
UP1	GAAGTCATCATGACCGTTCTGCAYGCNG GNGGNAARTTYGA	Partial *gyrB* gene amplification
UP2R	AGCAGGGTACGGATGTGCGAGCCRTCN ACRTCNGCRTCNGTCA	
*Zm_TEF-1α*_F	TGGGCCTACTGGTCTTACTACTGA	Relative biomass (endogenous control of plants)
*Zm_TEF-1α*_R	ACATACCCACGCTTCAGATCCT	
*Fv_β-tubulin*_F	CCCCGAGGACTTACGATGTC	Relative biomass (fungi)
*Fv_β-tubulin*_R	CGCTTGAAGAGCTCCTGGAT	
*Bv_gyrB*_F	CGTACGGTTCACAGGGACAG	Relative biomass (bacteria)
*Bv_gyrB*_R	ACACGGCCTTGGATCGTATG	

Note: R = A/G, Y = C/T, N = A/G/C/T